

Understanding the mechanisms for tropical surface impacts of the quasi-biennial oscillation (QBO)

Jorge Luis Garcia-Franco^{1,2}, Lesley J Gray³, Scott M. Osprey³, Robin Chadwick⁴, and Jonathan Lin²

¹University of Oxford

²Lamont-Doherty Earth Observatory, Columbia University, New York

³NCAS-Climate, Department of Physics, Oxford University

⁴Met Office

January 17, 2023

Abstract

This study evaluates the main hypotheses to explain a coupling between the quasi-biennial oscillation (QBO) in the tropical stratosphere and the tropical troposphere and surface. The impact of the QBO on tropical convection and precipitation is investigated through nudging experiments using the UK Met Office Hadley Centre Unified Model (UM). The model control simulations show robust links between the internally generated QBO and tropical precipitation and circulation. The model zonal wind in the tropical stratosphere was nudged above 90 hPa in atmosphere-only and coupled ocean-atmosphere configurations. The simulation of convection and precipitation in the atmosphere-only simulations is not statistically significantly different between the experiments with and without nudging, which may indicate that SST-convection coupling is needed for any QBO influence on the tropical lower troposphere and surface. In the coupled experiments, the precipitation and SST relationships with the QBO phase disappear when nudging is applied. Evidence from the nudging experiments shows that the QBO influence over lower stratospheric static stability is not sufficient to produce tropical surface impacts. The nudging also reduced the influence of the lower troposphere to the upper branch of the Walker circulation, irrespective of the QBO, indicating that the upper troposphere has been slightly decoupled from the surface by the nudging. These results suggest that nudging all grid-points might mute relevant feedback processes, including high cloud radiative effects and wave mean flow interactions, occurring at the tropopause level.

Understanding the mechanisms for tropical surface impacts of the quasi-biennial oscillation (QBO)

Jorge L. García-Franco^{1,2}, Lesley J. Gray^{1,3}, Scott Osprey^{1,3}, Robin Chadwick^{4,5} and
Jonathan Lin²

¹Atmospheric, Oceanic and Planetary Physics, University of Oxford

²Lamont-Doherty Earth Observatory, Columbia University, NY

³National Centre for Atmospheric Science, Oxford, United Kingdom

⁴Met Office Hadley Centre, UK

⁵Global Systems Institute, Department of Mathematics, University of Exeter, Exeter, UK

Key Points:

- Nudging the zonal wind in the equatorial stratosphere affects tropical convection variability only in coupled ocean-atmosphere simulations.
- The impact of the quasi-biennial oscillation (QBO) on upper-level static stability is not sufficient to influence tropical precipitation.
- Interactions between upward wave propagation and upper-level clouds is the likely mechanism of QBO tropical teleconnections.

Corresponding author: Lesley J. Gray, lesley.gray@physics.ox.ac.uk

Abstract

This study evaluates the main hypotheses to explain a coupling between the quasi-biennial oscillation (QBO) in the tropical stratosphere and the tropical troposphere and surface. The impact of the QBO on tropical convection and precipitation is investigated through nudging experiments using the UK Met Office Hadley Centre Unified Model (UM). The model control simulations show robust links between the internally generated QBO and tropical precipitation and circulation. The model zonal wind in the tropical stratosphere was nudged above 90 hPa in atmosphere-only and coupled ocean-atmosphere configurations. The simulation of convection and precipitation in the atmosphere-only simulations is not statistically significantly different between the experiments with and without nudging, which may indicate that SST-convection coupling is needed for any QBO influence on the tropical lower troposphere and surface. In the coupled experiments, the precipitation and SST relationships with the QBO phase disappear when nudging is applied. Evidence from the nudging experiments shows that the QBO influence over lower stratospheric static stability is not sufficient to produce tropical surface impacts. The nudging also reduced the influence of the lower troposphere to the upper branch of the Walker circulation, irrespective of the QBO, indicating that the upper troposphere has been slightly decoupled from the surface by the nudging. These results suggest that nudging all grid-points might mute relevant feedback processes, including high cloud radiative effects and wave mean flow interactions, occurring at the tropopause level.

Plain Language Summary

The interaction between the stratosphere and the troposphere is well known to produce surface impacts in the extratropics. However, whether stratosphere-troposphere interactions affect the surface in the tropics associated with the variability of the stratospheric quasi-biennial oscillation (QBO) is yet to be determined because the observational record is too short and tropical tropospheric variability masks any potential signal of the stratosphere. In this paper, we examine hypotheses that suggest the stratospheric quasi-biennial oscillation can affect tropical deep convection to the extent of influencing tropical surface precipitation variability through targeted model experiments which prescribe the equatorial stratosphere towards observations. Our results indicate that prescribing the zonal wind in the stratosphere remove links between surface precipitation and the QBO. The weight of the evidence in our findings suggest that the impact of the QBO on the static stability at the interface of the QBO and tropical convection is not enough

to produce significant effects over tropical convection and precipitation but high clouds in the tropics could play a bigger role than previously thought.

1 Introduction

The stratospheric quasi-biennial oscillation (QBO) has been linked to tropical deep convection for several decades (W. M. Gray, 1984; Giorgetta et al., 1999; Collimore et al., 2003; Liess & Geller, 2012). Observations show that the magnitude and location of tropical precipitation and several cloud properties are statistically related to the QBO phase (Liess & Geller, 2012; Tseng & Fu, 2017; L. J. Gray et al., 2018; H. Kim, Son, & Yoo, 2020; Hitchman et al., 2021; García-Franco et al., 2022; Sweeney et al., 2022). However, the extent to which the tropical troposphere and stratosphere are coupled, as well as the mechanisms that connect these two layers, remain a matter of debate (Haynes et al., 2021; Hitchman et al., 2021; Martin et al., 2021b).

Firstly, the relatively short observational record which limits our ability to detect any robust response of tropical precipitation to the QBO phase (Hu et al., 2012; García-Franco et al., 2022). The strong influence of El Niño-Southern Oscillation (ENSO) over tropical variability on interannual timescales is also a limiting factor for the attribution of anomalies in the tropics to the QBO (Liess & Geller, 2012; L. J. Gray et al., 2018; J.-H. Lee et al., 2019), especially because the ENSO-QBO relationship appears to have changed between 1960-1985 and 1985-2020 (Domeisen et al., 2019; García-Franco et al., 2022).

Secondly, there is no clear understanding of how the QBO could modulate tropical deep convection. Several hypotheses have been suggested to potentially explain a coupling of the QBO and the tropical troposphere including static stability (e.g. Nie & Sobel, 2015; Haynes et al., 2021), vertical wind shear (e.g. W. M. Gray et al., 1992), a QBO-Walker circulation feedback (Collimore et al., 2003; Hu et al., 2012; Hitchman et al., 2021; García-Franco et al., 2022) and cloud feedback hypotheses (Sakaeda et al., 2020). However, there is no clear understanding which of these hypotheses, if any, is the primary mechanism for a downward impact from the QBO on tropical convection.

The static stability hypothesis suggests that the meridional circulation driven by the descending QBO shear impacts the static stability in the region of the upper troposphere-lower stratosphere (UTLS; W. M. Gray et al., 1992; Giorgetta et al., 1999; Collimore et al., 2003; Liess & Geller, 2012; Nie & Sobel, 2015; Back et al., 2020). These studies argue that decreased UTLS static stability is found under the easterly phase (QBOE) compared to the westerly phase (QBOW),

79 leading to enhanced convection under QBOE (Collimore et al., 2003) which could explain, e.g.,
80 the stronger convection associated with the Madden-Julian Oscillation (MJO) under QBOE con-
81 ditions (Yoo & Son, 2016; Son et al., 2017; Hendon & Abhik, 2018; Back et al., 2020).

82 Observational and modelling results indicate that the QBO impact in the tropics is not zon-
83 ally symmetric (Collimore et al., 2003; Liess & Geller, 2012; García-Franco et al., 2022). For this
84 reason, several studies have suggested an interaction between the QBO and the Walker circula-
85 tion (Liess & Geller, 2012; Hu et al., 2012; Hitchman et al., 2021). Observations show that the
86 Walker circulation was weaker under QBOW compared to QBOE in the period of 1979-2021 (Hitch-
87 man et al., 2021; García-Franco et al., 2022) but the causal direction of this relationship remains
88 to be well understood.

89 A different hypothesis, however, suggests that cloud-radiative effects (CREs) associated with
90 the variability of tropical upper-level cirrus clouds explain the QBO-MJO link (Sun et al., 2019;
91 Sakaeda et al., 2020; Martin et al., 2021b; Lim & Son, 2022; Lin & Emanuel, 2022). Given the
92 importance of cirrus clouds for the radiative budget in the tropics due to their longwave CRE
93 (Allan, 2011; Hartmann & Berry, 2017) and the role of the QBO modulating variability of clouds
94 in the tropical tropopause layer (TTL) on interannual timescales (Liess & Geller, 2012; Davis et
95 al., 2013; Tseng & Fu, 2017; Tegtmeier et al., 2020; Sweeney et al., 2022), the QBO could rea-
96 sonably affect convection through CRE at different scales. Evidence for this hypothesis has shown
97 that more high-cloud coverage associated with the MJO is observed during QBOE compared to
98 QBOW (Sun et al., 2019; Sakaeda et al., 2020), suggesting that CREs associated with the QBO
99 could be a relevant mechanism for QBO tropical teleconnections. In short, despite the growing
100 number of hypotheses that explain a potential link between the QBO and tropical convective fea-
101 tures, a clear mechanism remains to be determined.

102 Since observations and theory have not successfully identified the mechanism for QBO tropi-
103 cal teleconnections, several studies have turned to numerical models such as cloud-resolving mod-
104 els (Nie & Sobel, 2015; Martin et al., 2019; Back et al., 2020) and General Circulation Models
105 (GCMs; J. C. K. Lee & Klingaman, 2018; H. Kim, Caron, et al., 2020; Serva et al., 2022) to iden-
106 tify pathways of stratospheric-tropospheric coupling. Although GCMs are more comprehensive,
107 stratospheric and tropospheric biases have hindered the potential use of these models to tackle
108 this problem because GCMs underestimate the amplitude of the QBO in the lowermost strato-
109 sphere (Fig. S1 and J. C. K. Lee & Klingaman, 2018; H. Kim, Caron, et al., 2020; Martin et al.,
110 2021a). For this reason, the variability of the UTLS static stability associated with the QBO is

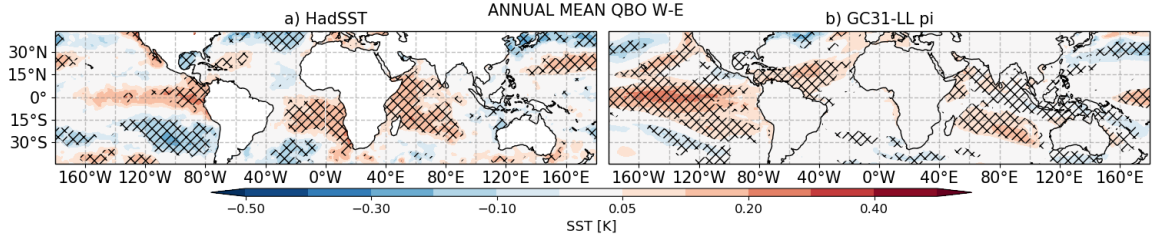


Figure 1. Annual mean SST [K] QBO W-E differences in (a) HadSST dataset and (b) the pre-industrial control simulation of the UM GC31-LL pi. Hatching denotes significance to the 95% confidence level.

111 lower than observed in models (Schenzinger et al., 2017; J. C. K. Lee & Klingaman, 2018; Bushell
 112 et al., 2020; Richter et al., 2020; Rao et al., 2020).

113 This weak amplitude bias in the QBO has been hypothesized to explain why some observed
 114 teleconnections, including the MJO-QBO relationship, are not diagnosed in GCMs (J. C. K. Lee
 115 & Klingaman, 2018; H. Kim, Caron, et al., 2020; Martin et al., 2021a). Due to these biases, sev-
 116 eral studies have performed or suggested experiments in which the model stratosphere is relaxed
 117 towards an observed or idealized state of the stratosphere, also known as nudging (e.g. Garfinkel
 118 & Hartmann, 2011; J. C. K. Lee & Klingaman, 2018; Richter et al., 2020; Martin et al., 2021a).
 119 The nudging technique can remove biases, identify causal pathways and test specific hypothe-
 120 ses to understand mechanisms (L. Gray et al., 2020; Haynes et al., 2021).

121 This study aims to understand QBO tropical teleconnections by addressing the issue of QBO
 122 model biases using relaxation experiments of the Met Office Hadley Centre (MOHC) Unified Model
 123 (UM). The UM is a state-of-the-art GCM that is able to simulate an internally generated QBO
 124 that is reasonably similar to observations, except for the weak amplitude bias in the lower strato-
 125 sphere (Richter et al., 2020). In addition, nudging has previously been successfully applied in this
 126 model (Telford et al., 2008; L. Gray et al., 2020). The UM exhibits robust connections between
 127 the tropical troposphere associated with the QBO, which are described in García-Franco et al.
 128 (2022), including a sea-surface temperature (SST) signal (see Figure 1) that is similar to the ob-
 129 served record and El Niño events occur more frequently under QBOW compared to QBOE.

130 The main purpose of this study is to evaluate the effect of nudging on the representation
 131 of the QBO surface impacts in the tropics. The results of these experiments will be used to crit-
 132 ically examine existing hypotheses suggested to explain QBO-convection links: the static stabil-

133 ity mechanism and QBO-Walker circulation relationships, and the role of CREs. The remain-
134 der of this paper is presented as follows. Section 2 describes the nudging experiments, as well as
135 the observations, CMIP6 and reanalysis datasets used to compare the experimental results. Sec-
136 tion 3 presents the results of the experiments. The final section presents a discussion and con-
137 clusions arising from this study.

138 **2 Methods and data**

139 **2.1 Observations and reanalysis**

140 Observational data of precipitation and SSTs are used in this study. The Global Precip-
141 itation Climatology Project (GPCP) v2.3 (Adler et al., 2003) dataset is used for precipitation
142 analyses and the HadSST v4.0 (Kennedy et al., 2019) for SST. For the remaining diagnostics,
143 including the zonal wind and convective precipitation we use the reanalysis ERA5 from the Eu-
144 ropean Centre for Medium-Range Weather Forecasts (ECMWF) (Hersbach et al., 2020) down-
145 loaded at the $0.75 \times 0.75^\circ$ resolution from <https://cds.climate.copernicus.eu/cdsapp>. In all
146 cases the data cover the period 1979-2021.

147 **2.2 The Met Office Unified Model**

148 The MOHC UM uses a seamless approach modelling framework that allows the setup of
149 simulations using various configurations; for example, various horizontal resolutions maintain-
150 ing the same parametrizations and dynamical core (Walters et al., 2019). In addition to the main
151 experimental design for nudging used in this study, which is explained in detail in the following
152 section, the CMIP6 preindustrial control experiment from the MOHC model HadGEM3 is used
153 for comparison. The preindustrial control experiments use constant external forcing integrated
154 for 500 years (Menary et al., 2018). In this study we use results from the HadGEM3 GC3.1 N96
155 (GC31-LL) experiment.

156 **2.3 Nudging scheme**

157 Nudging refers to the relaxation of a model variable towards a specified state, which can
158 be taken from reanalysis, observations or idealized states (L. Gray et al., 2020; Martin et al., 2021a).
159 In the UM setup, three variables can be nudged: air temperature (T) and the zonal (u) and merid-
160 ional (v) components of the wind; in this study we use ERA5 as the nudging data. The relax-
161 ation is applied at each grid-point, in contrast to other studies (e.g. Martin et al., 2021a) that

162 employ a spectral model and apply the relaxation only to the zonal-mean component. Specif-
 163 ically, the UM uses a Newtonian relaxation technique (Telford et al., 2008; L. Gray et al., 2020)
 164 which sets the field to be nudged (F) at each time-step through the following equation:

$$\Delta F = G\Delta t(F_{ndg} - F_{model}), \quad (1)$$

165 where ΔF is the discrete change of F at each time-step, G is the relaxation parameter, Δt is the
 166 time-step size, F_{ndg} is the value of the field from the nudging data and F_{model} is the model value
 167 of the field at the last time-step (Telford et al., 2008).

168 The relaxation parameter G sets the strength of the relaxation and is linked with the re-
 169 laxation timescale (τ) by $G = 1/\tau$. Previous studies (Telford et al., 2008; L. Gray et al., 2020)
 170 have shown that a 6-h relaxation time-scale is sufficient to constrain the stratosphere in the model
 171 and so the same parameter was used for the simulations of this chapter ($G = \frac{1}{6} \text{ h}^{-1}$).

172 Furthermore, the nudging can be performed between specified vertical levels and in selected
 173 latitude/longitude regions with *tapering*, which refers to a linear interpolation between the max-
 174 imum G and zero nudging ($G = 0$). The chosen experimental design relaxes only the zonal wind
 175 (u) at all longitudes in the latitude band of 20°S-20°N, with a 10° tapering, at the model lev-
 176 els corresponding to 90 hPa to 4 hPa, with a vertical tapering of 4 levels, which means that full
 177 nudging was in effect only at 10°S-10°N from 70 hPa to 10 hPa. The experimental setup aims
 178 to reasonably simulate the observed variability of the zonal wind leaving the meridional compo-
 179 nent of the wind and the temperature to respond freely within the model.

180 2.4 Experimental design

181 The configuration of the UM model used for the nudging experiments is GC3.1 (version 11.4),
 182 which is the same configuration as the CMIP6 experiments (Walters et al., 2019). All the exper-
 183 iments, AMIP and coupled, are set up using a present-day climate configuration where all ex-
 184 ternal forcings are set constant to those of the year 2000. The atmospheric horizontal resolution
 185 is N96 (1.875°x1.25°) for our experiments. A summary of all the experiments is given in Table
 186 1.

187 The atmosphere-only (AMIP) experiments were conducted for 32 years (1981-2012) using
 188 prescribed SST and sea-ice boundary conditions for the period 1981-2012, using the data pro-
 189 vided as part of the CMIP6 AMIP forcing setup. Three sets of AMIP experiments were run: Con-

Table 1. Experimental setup indicating the model configuration, the period, number of ensemble members (Ens.) and relaxation details.

Name	Configuration	Period	Ens.	Nudging
AMIP	Atmosphere-only	1981-2012	3	ERA5.
AMIP-Control	Atmosphere-only	1981-2012	3	No nudging
AMIP-Shifted	Atmosphere-only	1981-2012	3	ERA5 Relaxation shifted -1 year.
Coupled Nudged	Coupled ocean-atmosphere	1981-2015	6	ERA5.
Coupled Control	Coupled ocean-atmosphere	1981-2015	6	No nudging

190 trol, Nudged and Shifted. In the control experiment, the model stratosphere was free to evolve.
 191 In the Nudged experiment, the equatorial zonal wind was nudged, as described in the previous
 192 section, with the nudging wind data matching the corresponding SST data.

193 In addition, we performed another type of atmosphere-only experiment, the Shifted exper-
 194 iment. In the normal AMIP Nudged experiment, the SST driving data corresponds to the same
 195 year as the nudged zonal wind in the equatorial stratosphere. In the Shifted experiment, the nudg-
 196 ing data was shifted with a -1 year lag from the SSTs, e.g., the model year 1997 was run using
 197 1997 SSTs but zonal winds in the stratosphere corresponding to 1996. An alternative approach
 198 would be to *shuffle* the SSTs so that each year is run with randomly selected SSTs. However,
 199 since we are performing multi-year simulations shuffling has associated issues of how to join the
 200 randomly-selected SSTs at the year-boundary to form a coherent multi-year SST time-series. To
 201 avoid this issue we decided to simply shift the zonal wind nudging data by one year so the QBO
 202 phase and SSTs were not aligned.

203 For the coupled ocean-atmosphere experiments, a control and a nudged ensemble of 6 mem-
 204 bers were run for 35 years (1981-2015 model years). The coupled experiments use an oceanic res-
 205 olution of 0.25° (ORCA025) using the NEMO model (Storkey et al., 2018). Each ensemble mem-
 206 ber was initialized from different ocean/atmosphere initial conditions, in order to decrease the

207 role that internal variability may have on these simulations by averaging out the ensemble. Specif-
208 ically, the coupled ocean-atmosphere configuration was initialized using oceanic conditions from
209 a 100-yr simulation of the same model configuration that were found 10 years apart from each
210 other.

211 2.5 Indices and methods

212 ENSO is measured through the standard Oceanic Niño Index, i.e., the time-series of area-
213 averaged SSTs in the Niño 3.4 region (hereafter EN3.4 Trenberth, 1997) and a 5-month running
214 mean using a 0.5 K threshold to define positive or negative events. The QBO index is defined
215 using the equatorially-averaged [10S-10N] zonal winds at the 70 hPa level and a $\pm 2 \text{ m s}^{-1}$ thresh-
216 old to define W and E phases. A measure of the zonal gradient of convective activity in the In-
217 dian Ocean is used as a proxy of the Indian Ocean Dipole (IOD), as in García-Franco et al. (2022).
218 Composite and regression analysis are used to evaluate the differences amongst experiments, as
219 in García-Franco et al. (2022). Statistical significance in observations and individual ensemble
220 members is diagnosed using a bootstrapping method with replacement, whereas for all ensemble-
221 mean differences, given their relative larger sample size, standard two-sided t-tests are used.

222 3 Results

223 Figure 2 demonstrates that nudging increases the UTLS temperature and zonal wind vari-
224 ability associated with the QBO. The comparison of the QBO W-E difference between the nudged
225 experiments, ERA5, the 500-yr CMIP6 GC31-LL simulation, and the control experiments shows
226 that the nudged experiments closely resemble the results from ERA5 whereas the control exper-
227 iments exhibit a much weaker signal. In the tropical UTLS region, the nudged experiments show
228 a wider and stronger QBO signal than the control experiments which demonstrates that these
229 experiments are suitable to explore the processes that relate the QBO with the tropical surface.
230 The control-nudged difference plots (Fig. S2) illustrate that the warm anomalies near the equa-
231 torial tropopause between 70-90 hPa are up to 1.5 K larger in the nudged experiments.

232 Since the nudging technique has removed the weak QBO amplitude bias in the lower strato-
233 sphere, we now analyse tropical teleconnections in these experiments. First, results from the atmosphere-
234 only experiments are analysed, followed by the analysis of the coupled experiments. The final
235 section investigates the mechanisms that could explain the differences between nudged and con-
236 trol experiments.

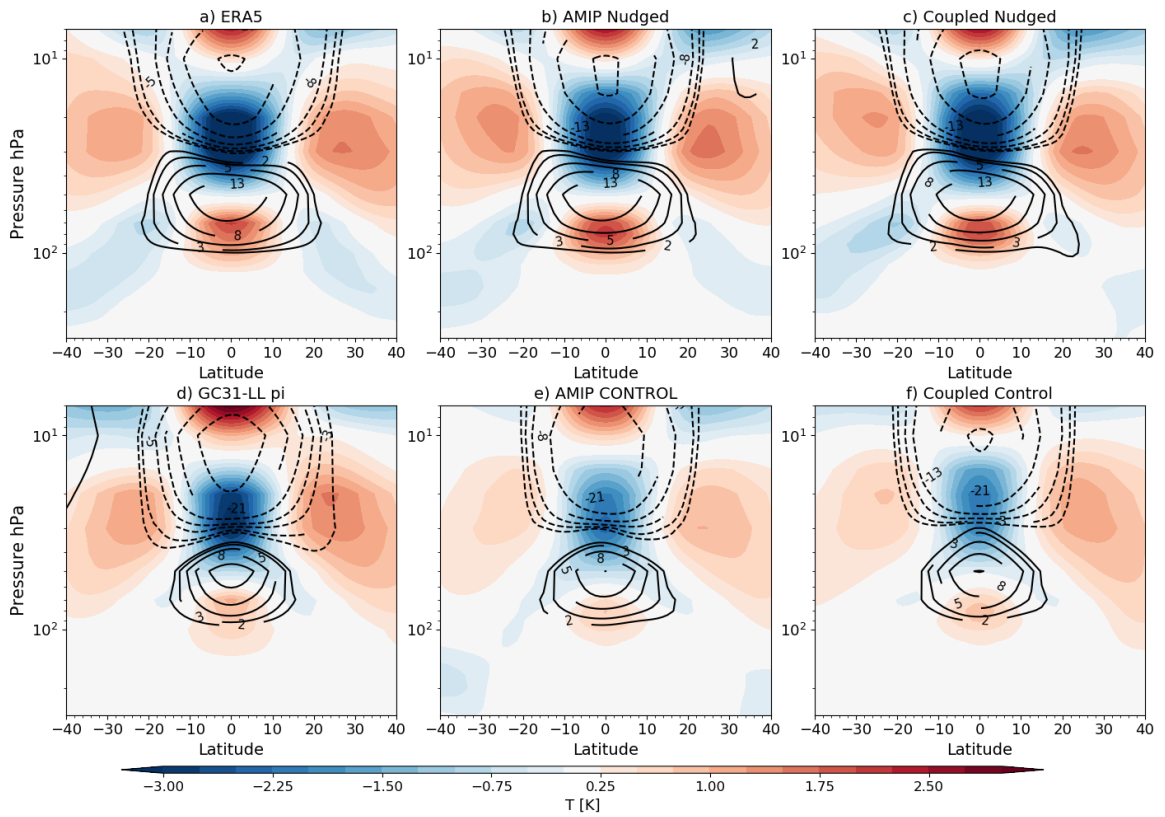


Figure 2. Latitude-height plot of the zonal-mean temperature (shading) zonal wind (contours in m s^{-1}) QBO W-E differences in (a) ERA5, the nudged simulations in (b) AMIP and (c) coupled configurations and (d) GC31 N96-pi from CMIP6, the control simulations with no nudging in an (e) AMIP and (f) coupled configurations

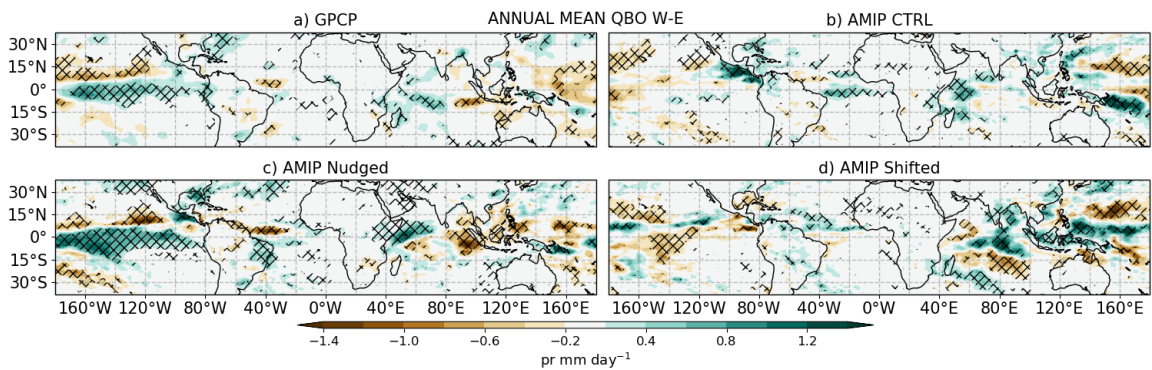


Figure 3. Annual-mean precipitation response (QBO W-E) in (a) GPCP, and atmosphere-only experiments: (b) AMIP CTRL, (c) AMIP Nudged and (d) AMIP Shifted.

238 This section shows the results of the atmosphere-only experiments: AMIP Nudged, AMIP
 239 Control and AMIP Shifted (in which the imposed winds have been shifted by a year so there is
 240 an out-of-phase relaxation of the winds with respect to the SSTs), compared to observations (1981-
 241 2012). The annual-mean difference of precipitation between QBOW and E phases from the three
 242 experiments are compared with GPCP differences in Fig. 3. The AMIP Nudged ensemble-mean
 243 matches closely the results of GPCP, characterised by an El Niño pattern in the Pacific Ocean,
 244 a weaker Atlantic ITCZ and a zonal gradient of precipitation in the Indian Ocean during QBOW
 245 compared to QBOE.

246 In contrast, the differences in the AMIP Control and the AMIP Shifted experiments show
 247 little similarity to the observed response, a similar result is found for seasonal-mean composite
 248 differences (see e.g. Fig S3). The fact that the QBO response is different in the three types of
 249 AMIP experiments suggests that the underlying SSTs, and not the QBO winds, are responsible
 250 for these differences. However, it may still be the case that tropical convection is sensitive to the
 251 QBO phase in these simulations and this effect is hidden by the strong effect of SST forcing.

252 Time-series of multiple diagnostics averaged at equatorial latitudes and in the EN3.4 re-
 253 gions are shown in Figure 4. The tropical mean outgoing longwave radiation (OLR) and precip-
 254 itation is not significantly affected by the nudging, suggesting that convective activity is inde-
 255 pendent from the state of the QBO at 70 hPa. The correlation coefficients of precipitation and
 256 OLR with respect to observations (a-b) are indistinguishable between experiments, both for the
 257 tropics-wide (a, c) and for the EN3.4 region (b, d).

258 The timeseries of the equatorial zonal mean zonal wind at 70 hPa (U_{70} ; Fig. 4e) shows a
 259 correlation between ERA5 and the Nudged experiment, as expected. In contrast, the correlation
 260 of ERA5 with AMIP CTRL is virtually zero, because the ensemble-mean zonal wind of the CTRL
 261 collapses to near zero values. The Shifted experiment shows a negative and high correlation (0.65)
 262 with ERA5, which is not surprising, since the SSTs have been shifted by one year i.e. approx-
 263 imately half a QBO cycle.

264 The timeseries of the near-tropopause temperature (T_{100} ; Fig. 4g-h) shows that the Nudged
 265 ensemble is correlated with ERA5 in the tropical mean. This correlation increases for the EN3.4
 266 region in all the experiments such that the three simulations are well correlated with ERA5, al-
 267 though the Shifted experiment shows the lowest correlation. These results suggest the near-tropopause
 268 temperature is controlled by the QBO in the zonal-mean but by local SSTs at regional scales.
 269 In short, this section shows that in atmosphere-only experiments the nudging produces the ex-

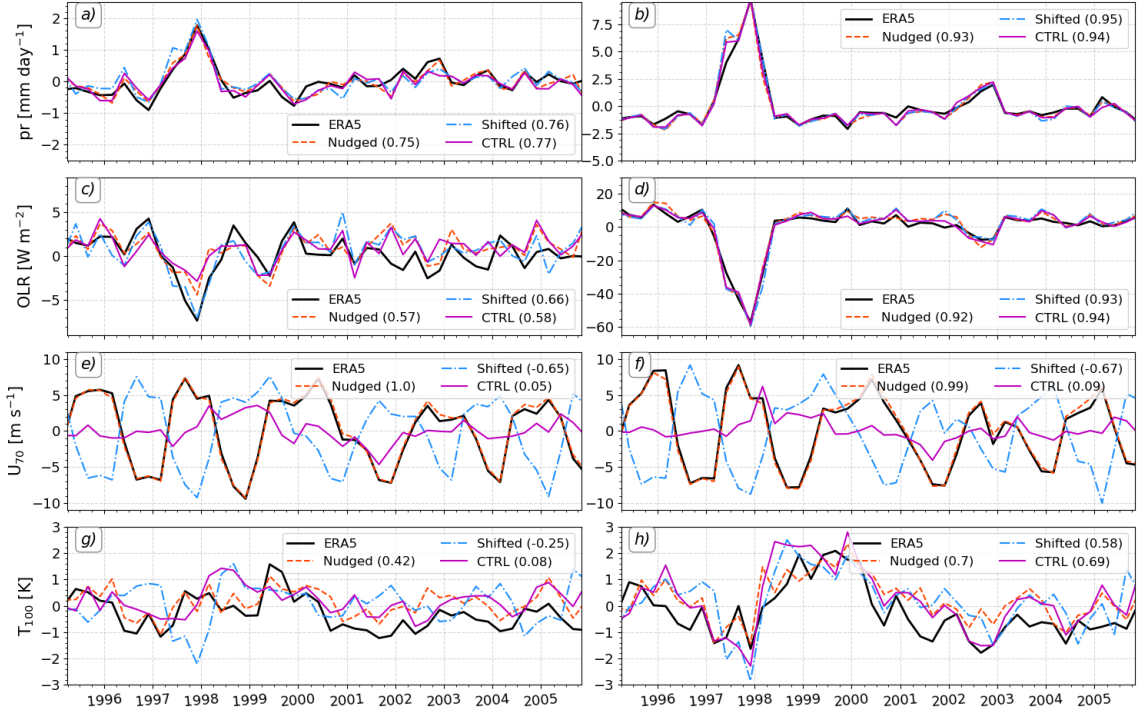


Figure 4. Time-series in the atmosphere-only experiments of (a, b) precipitation, (c, d) outgoing longwave radiation (OLR), (e, f) zonal wind at 70 hPa (U_{70}) and (g, h) air temperature at 100 hPa. The timeseries are shown for quantities averaged over the (left) zonal-mean equatorial $[5^{\circ}\text{S}-5^{\circ}\text{N}]$ and (right) EN3.4 regions. For each AMIP experiment the Pearson correlation coefficient between the experiment and ERA5 is shown in the legend. Note that the model year refers to the SST years as described in section 22.4.

270 expected impacts in U_{70} and the zonal-mean T_{100} , however, the nudging appears to have no made
 271 impact on the simulation of precipitation and OLR.

272 3.2 Coupled experiments

273 This section analyses the coupled ocean-atmosphere experiments, labelled as the Coupled
 274 Nudged and the Coupled Control simulations, which consist of 6 ensemble members (see section
 275 22.4). The SST response is first examined through the annual mean QBO W-E ensemble-mean
 276 difference in tropical SSTs of the coupled control experiments (Fig 5a-b) which compares rea-
 277 sonably well with the results from HadSST and GC3 LL-pi (Fig. 1). This response is character-
 278 ized by warmer SSTs (+0.2-0.3K) during QBOW than during QBOE in the deep tropics and gener-
 279 ally cooler subtropical oceans. However, for the Coupled Nudged ensemble-mean, the tropi-

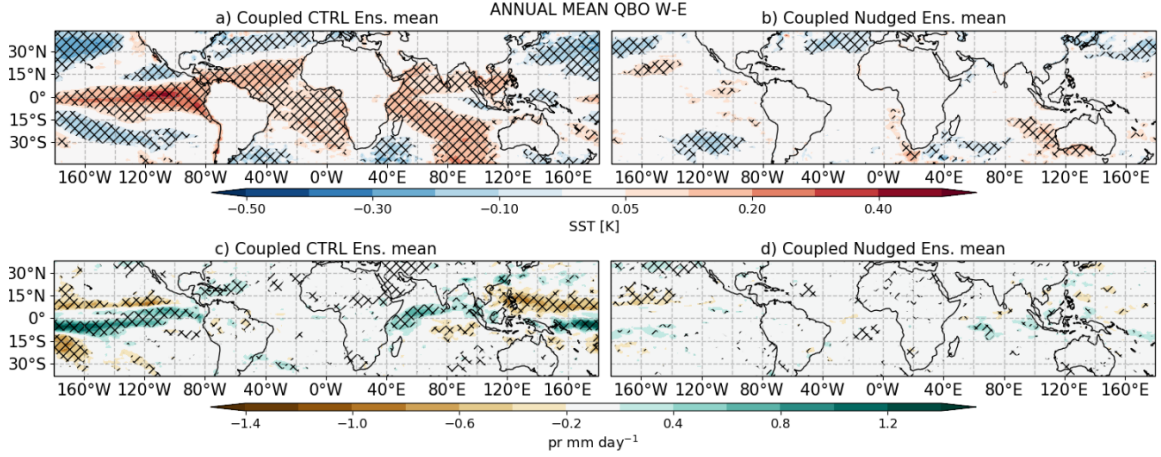


Figure 5. As in Fig. 1 but for results of the (a, c) Coupled Control and (b, d) Coupled Nudged ensemble-mean (a, b) SST [K] and (c, d) precipitation [mm day^{-1}].

280 cal response is essentially zero, although some sparse regions showing slight cooling (W-E) can
 281 be observed in the subtropics. This means that the nudging has affected the physical mechanism
 282 behind the robust statistical relationship between the tropical SSTs and the QBO phase in the
 283 UM (García-Franco et al., 2022).

284 The QBO W-E differences in each of the 6 ensemble members in the Control and Nudged
 285 experiments (Fig. S4) show that the weak response in the ensemble-mean of the nudging exper-
 286 iments is the result of very different responses from each ensemble member. These individual re-
 287 sponses cancel out to a large extent. In contrast, most of the control ensemble members exhibit
 288 a warming signal in the equatorial oceans, leading to the statistically significant response seen
 289 in the ensemble-mean.

290 The precipitation response (Fig. 5c-d) follows closely the SST patterns. The robust rela-
 291 tionship between the QBO and tropical precipitation in the UK UM (García-Franco et al., 2022)
 292 is also observed in the Control experiment characterized by shifts of the ITCZ in the Pacific and
 293 Atlantic sectors and a wetter western Indian Ocean. This relationship is, however, removed, when
 294 the nudging is applied as the nudged ensemble-mean is virtually zero across the tropics, which
 295 is also due to the cancelling effect of different responses in individual ensemble members (Fig.
 296 S5).

297 One key result from García-Franco et al. (2022) was a robust relationship between the QBO
 298 and the IOD during boreal fall. Figure 6 shows that this relationship is also robust in the Con-

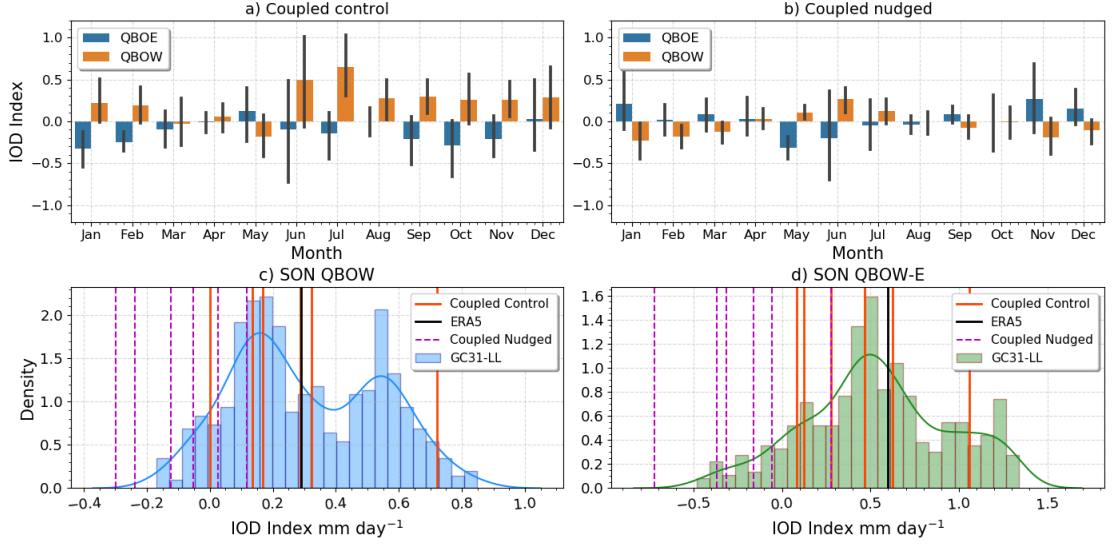


Figure 6. (a, b) Monthly-mean convective precipitation IOD index [mm day⁻¹] in coupled (a) control and (b) nudged ensemble-means separated by QBO phase; the error bars indicate ensemble spread. (c, d) Probability density functions (PDFs) of the IOD convective precipitation index for (c) the mean SON during QBOW months and (d) the SON difference between QBO W-E. The PDF is obtained by bootstrapping the 500 yr simulation of the GC31-LL 42-yr periods and obtaining the averages and differences in each sub-sample. The mean values for the Coupled Control and Nudged experiments, as well as for ERA5 are shown as vertical lines.

299 control experiments of this configuration but not in the Coupled Nudged experiments. A probabil-
 300 ity density function (PDF) of QBO W-E in the IOD index was constructed using 35-yr chunks
 301 of the pre-industrial control experiment GC31-LL to sample internal variability within the model.
 302 The difference in the IOD index per QBO phase for individual ensemble members from the Control
 303 and Nudged experiments is plotted together with the GC31-LL PDF (Fig. 6c-d) to exam-
 304 ine the likelihood that the results from the Nudged experiments happen by chance.

305 The results in Fig. 6c-d strongly suggest that the influence on the IOD is removed when
 306 nudging is applied given that some ensemble Nudged members show differences that are outside
 307 of the 99% range of the PDF whereas all the Control experiments show results that fall close to
 308 the median of the GC31-LL PDF. The results for the EN3.4 index are very similar (Supplemen-
 309 tary Fig. S6) confirming the ENSO-QBO relationship has been removed by the nudging.

310 This section shows that the coupled control experiments in our configuration broadly re-
 311 produce those of García-Franco et al. (2022), i.e., warmer SSTs and wetter conditions in the deep

312 tropics in QBOW compared to QBOE as well as statistical links between the QBO and ENSO
 313 and the IOD. However, nudging has significantly affected the relationships between the QBO and
 314 the tropical troposphere. Several plausible explanations, including the possibility that the sta-
 315 tistical relationships diagnosed by García-Franco et al. (2022) are simply due to an upward ef-
 316 fect from the troposphere to the stratosphere, are discussed in the final section. The following
 317 section evaluates three hypotheses using these experiments.

318 **3.3 Mechanisms**

319 The main mechanisms suggested by the literature to possibly explain a role for the QBO
 320 in modulating aspects of tropical convection are the static stability, QBO-Walker circulation and
 321 high-cloud effects. This section aims to evaluate these hypotheses through a comparison of the
 322 coupled nudged and Control experiments.

323 *3.3.1 The static stability hypothesis*

324 The effect of the QBO over the tropical UTLS temperature structure has been well doc-
 325 umented (Tegtmeier et al., 2020; Martin et al., 2021c) and is, arguably, the most frequently sug-
 326 gested mechanism that relates tropical convection variability to the QBO (Collimore et al., 2003;
 327 Liess & Geller, 2012; Hu et al., 2012; Nie & Sobel, 2015; J. C. K. Lee & Klingaman, 2018; Hitch-
 328 man et al., 2021). The UTLS static stability is defined here by the temperature difference (ΔT)
 329 between 150 and 70 hPa, so that negative values indicate decreased stability. Other definitions
 330 of ΔT such as the temperature difference between 250 hPa and 70 hPa, as well as using the 100
 331 hPa temperature field as a proxy yield similar results to our definition.

332 Figure 7 shows the QBO (W-E) signal in ΔT and convective precipitation. The spatial dis-
 333 tribution of the ΔT differences is relatively zonally symmetric, although for ERA5 and the nudged
 334 experiments ΔT maximizes in the Eastern Pacific. The magnitude of the QBO-related variabil-
 335 ity in ΔT is doubled by the nudging in the deep tropics compared to the control experiments,
 336 however the precipitation response is not increased in the nudged experiment. The precipitation
 337 response to the QBO in models and observations is, firstly, not zonally symmetric and secondly,
 338 not collocated with the largest influence of the QBO signal on the static stability differences.

339 The relationship between the UTLS static stability and tropical precipitation is investigated
 340 in more detail in Figure 8. This figure shows several scatter plots of the spatial and temporal re-
 341 lationship between the static stability and precipitation in both reanalysis and our model sim-

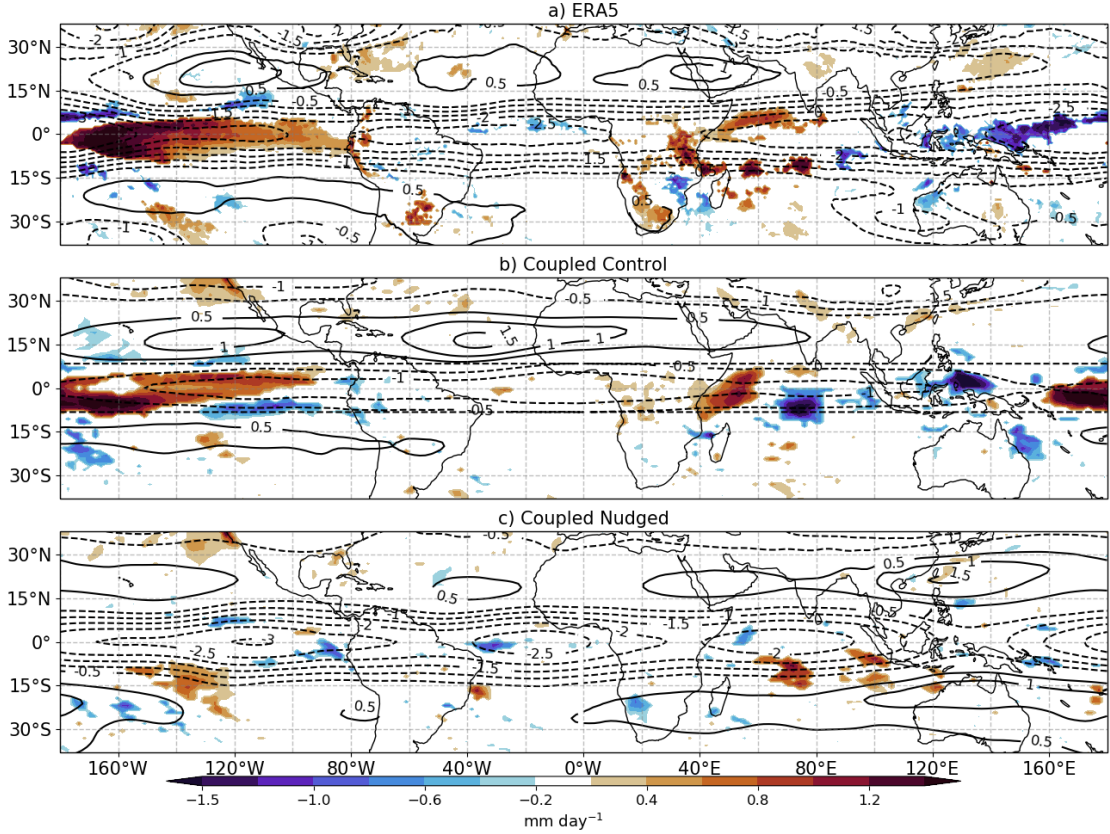


Figure 7. Convective precipitation (shading) and UTLS static stability (ΔT contours in [K]) DJF composite differences (QBO W-E) in (a) ERA5 and the ensemble-mean Coupled (b) Control and (c) Nudged experiments. Only statistically significant differences to the 95% confidence level are plotted.

342 ulations. First, Figure 8a shows the scatter plot of the monthly-averaged ΔT versus Δpr in the
 343 equatorial Western Pacific; such that each points represents a month in ERA5. Therefore, this
 344 figure shows that these two variables have a very weak temporal correlation. In other words, in
 345 ERA5, the temporal variability of the UTLS static stability is not related to precipitation vari-
 346 ability in the West Pacific warm pool. The sign of the correlation coefficient (weak in any case)
 347 reverses between QBOW months and QBOE months. Similar results are found for the simula-
 348 tions (not shown).

349 Next, Figure 8b shows a scatterplot of the annual mean QBO W-E differences of ΔT ver-
 350 sus Δpr at each grid-point in the Coupled nudged and Coupled Control experiments. The mag-
 351 nitude of the negative ΔT differences is higher in the nudged experiments than in the control whereas
 352 the spread of the precipitation differences is higher in the control. This figure illustrates that the
 353 nudging increases the spread of the ΔT differences but not of precipitation. Moreover, in the con-

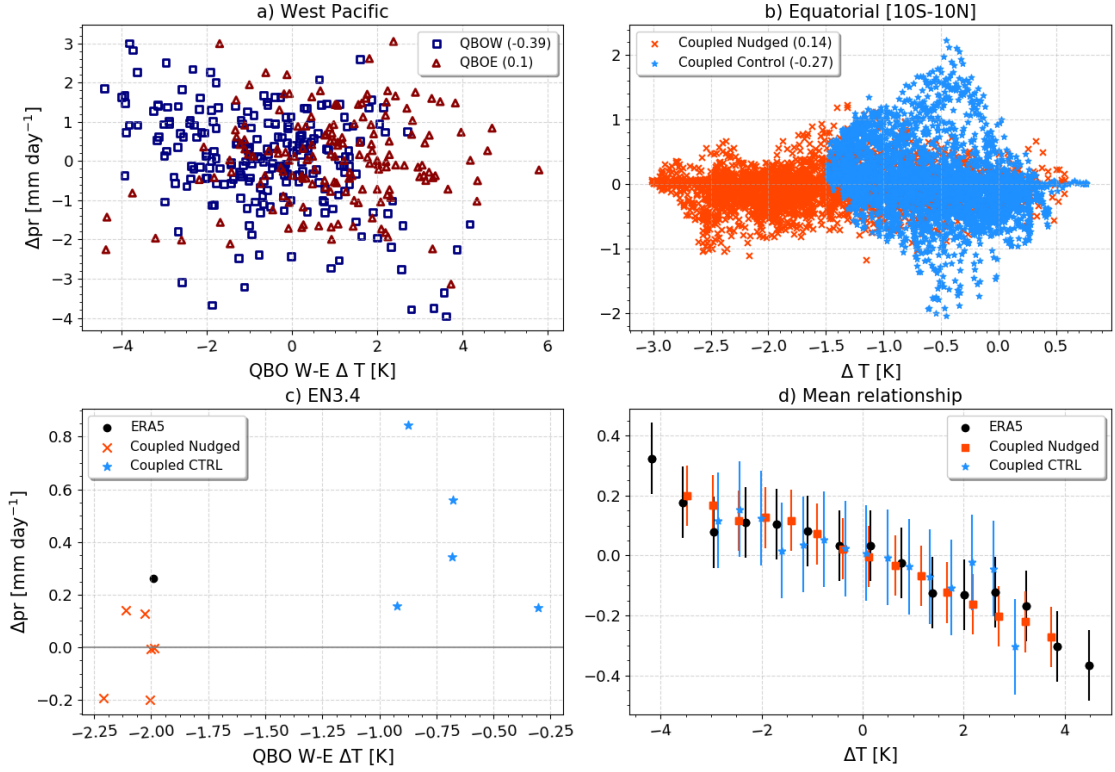


Figure 8. a) Scatter plot of deseasonalized convective precipitation [Δpr mm d⁻¹] versus UTLS static stability [ΔT K] anomalies for the western equatorial Pacific [0-10N,120-160E] in ERA5. Each data-point represents a month in the 1979-2021 period. b) As in a) but for the DJF ensemble-mean QBO W-E differences in the equatorial latitudes [10S-10N] in the simulations, so each dot represents a grid-point. c) Scatter plot of the annual-mean QBO W-E differences in Δpr versus ΔT in the EN3.4 region for each ensemble member of the simulations and ERA5. d) Mean relationship of Δpr versus ΔT computed by binning ΔT in all the grid-points at all times and computing the corresponding mean Δpr .

354 trol experiments, both positive and negative precipitation differences are found for similar ranges
 355 of ΔT differences. The existence of both positive and negative differences in Δpr for similar val-
 356 ues of ΔT in the control indicates that there is no unique longitudinally coherent or zonally sym-
 357 metric impact of the QBO. Additionally, this plot suggests that the magnitude of the precipi-
 358 tation differences are not explained by ΔT differences.

359 Then, Figure 8c shows how annual mean QBO W-E differences in ΔT are related to Δpr
 360 in the Niño3.4 region for each ensemble member of the control and nudged experiments. All the
 361 coupled control ensembles show a positive precipitation difference (W-E) of up to 0.85 mm day⁻¹,
 362 even though the static stability difference (W-E) is half as strong compared to the nudged ex-

363 periments. The nudged ensemble members, in contrast, simulate both positive and negative pre-
 364 cipitation responses close to 0, indicative of no statistical relationship between ENSO and the
 365 QBO in these experiments.

366 Finally, Figure 8d analyses the average relationship between ΔT and Δpr . In this plot, all
 367 the monthly-mean anomalies of convective precipitation and absolute values of ΔT have been
 368 composited using all the grid-points at equatorial latitudes [10°S-10°N] for all the months in each
 369 simulation. This procedure pairs Δpr and ΔT taken at the same time and space coordinates. From
 370 this composite, the average Δpr anomalies were computed for equally-separated bins of ΔT (start-
 371 ing at the 1th percentile and up to the 99th percentile). In this plot, the variability of ΔT is not
 372 necessarily associated with the QBO but the purpose of this plot is investigate whether precip-
 373 itation anomalies are related to the upper-level temperature structure more generally.

374 Therefore, Figure 8d shows the average precipitation anomaly for each ΔT bin. The mean
 375 relationship across the different datasets appears to be of a weak negative relationship which be-
 376 comes significant for high absolute values of ΔT characterized by higher static stability associ-
 377 ated with less precipitation and decreased UTLS static stability associated with more precipi-
 378 tation. This result would support the main assumption of the static stability mechanism, i.e.,
 379 that decreased upper level static stability associated with the QBO leads to more precipitation.
 380 This Figure also confirms that the nudging has increased ΔT variability but the nudging has only
 381 increased precipitation variability only for negative ΔT values.

382 The implication from these results is that nudging has increased ΔT variability and indeed
 383 UTLS static stability is linked to precipitation, however, the time-mean composite differences,
 384 shown in the previous section, suggest that these local-scale ΔT impacts are not enough to sim-
 385 ulate a time-mean significant signal on surface precipitation. In other words, this section presents
 386 evidence that in the UM and ERA5, QBO-related changes to static stability are not a sufficient
 387 factor to modulate tropical convection.

388 ***3.3.2 The Walker circulation***

389 Several studies have suggested a link between the QBO and the Walker circulation (Liess
 390 & Geller, 2012; Hitchman et al., 2021; García-Franco et al., 2022): specifically, in the UM the
 391 Walker circulation is weaker under QBOW than under QBOE. Figure 9 shows the impact of nudg-
 392 ing on the mean state and QBO-ENSO related variability of the Walker circulation. The biases
 393 in the mean-state of the Walker circulation are large in the control experiment, with differences

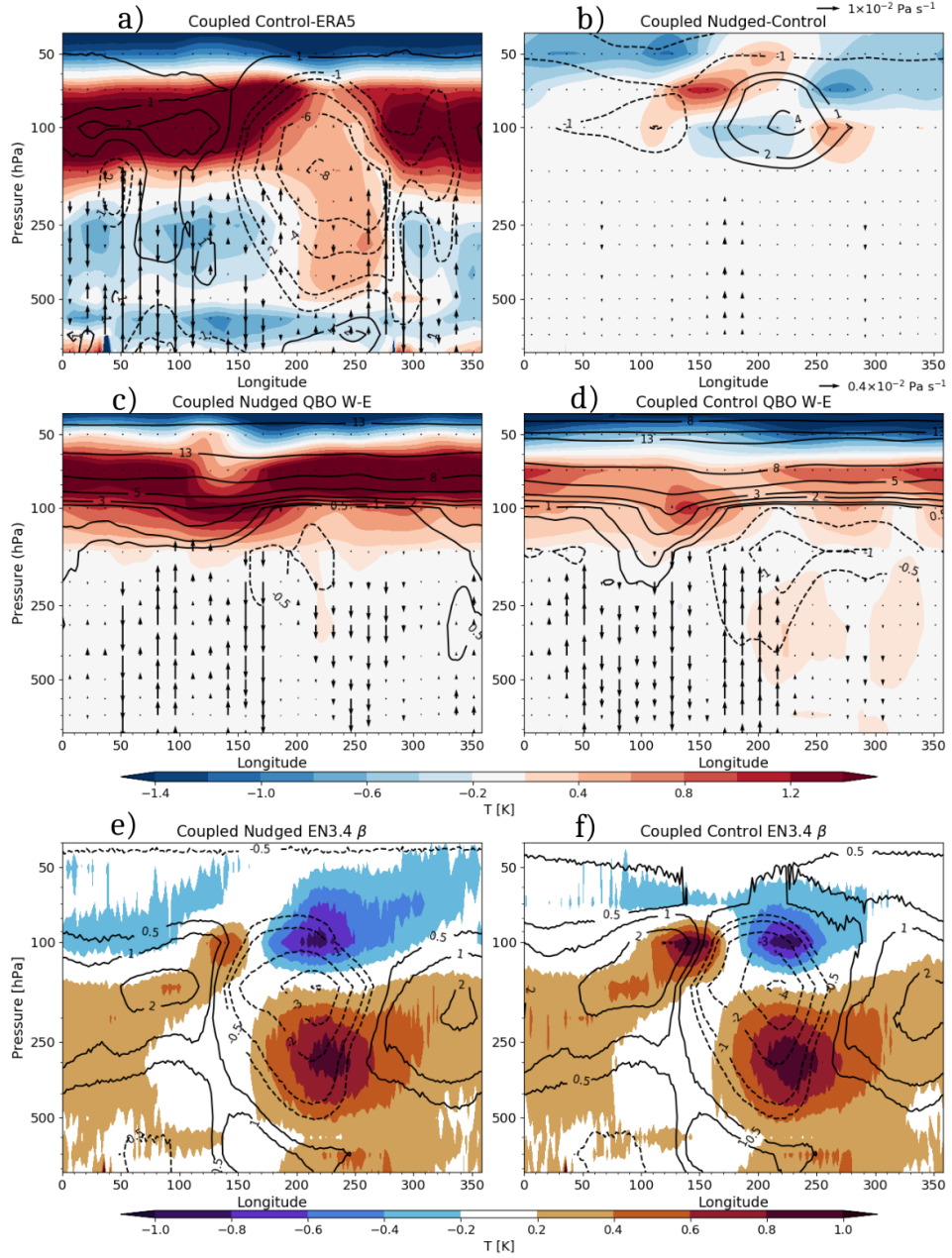


Figure 9. (a) Mean biases, diagnosed as differences between control ensemble-mean and ERA5, in the Walker circulation, (equatorial averages [10S-10N]) diagnosed from the zonal mean temperature (K in shading), zonal wind (contours in m s^{-1}) and vertical velocity (vectors in Pa s^{-1}). (b) shows the differences between nudged and Control coupled experiments. (c-d) show the QBO W-E differences for the (c) nudged and (d) Control ensemble-mean. (c-d) is as in (a-b) except that the (c-d) vector key is different than for (a-b). (e-f) show the results of the regression coefficients (β) between the zonal wind (contours) and the air temperature (shading) fields with the EN3.4 index.

394 of up to 6 m s^{-1} and 1.5 K compared to ERA5 (Fig. 9a). However, nudging improves some of
 395 the zonal wind biases (b), especially in the Pacific Ocean, while also producing an impact on UTLS
 396 temperature biases ($\approx 0.5 \text{ K}$).

397 The QBO-related Walker circulation variability appears to be affected by the nudging. In
 398 the upper troposphere, the QBO impact on the zonal wind and vertical velocities is different for
 399 nudged and control experiments (c versus d). This difference is more obvious in the Indian Ocean
 400 sector where the control experiments suggest that the W-E response is characterized by anoma-
 401 lous ascent in the western sector and descent in the eastern sector, yet the nudged response is
 402 the opposite.

403 Regression analysis was used to investigate the interaction of ENSO, the QBO and the Walker
 404 circulation, as in García-Franco et al. (2022). Figures 9e-f suggest that not only are the mean-
 405 state and the QBO relationships affected but the linear relationship between ENSO and the up-
 406 per branch of the Walker circulation is weakened when the nudging was applied (see e.g. 150E
 407 at 100 hPa where the temperature signal is twice as large in the control experiment). Note, how-
 408 ever, that the lower tropospheric ENSO signal remains unchanged.

409 These results suggest that the effect from ENSO on to the UTLS temperature has been weak-
 410 ened by the nudging which suggests that the nudging may have overly constrained the upper-
 411 branch of the Walker circulation. Feedback processes between convection and the UTLS tem-
 412 perature may have been reduced in strength and the temperature field, constrained through ther-
 413 mal wind balance, which are perhaps related to the nature of the nudging conducted in this study
 414 (see section 4 for a more detailed discussion on this possibility).

415 **3.3.3 The CRE hypothesis**

416 High cirrus CREs are a key aspect of tropical climate (Hartmann & Berry, 2017; Byrne &
 417 Zanna, 2020) such that recent studies have suggested mechanisms through which CREs explain
 418 the observed MJO-QBO connection (Sun et al., 2019; Lin & Emanuel, 2022; Lim & Son, 2022).
 419 This section uses model diagnostics that are relevant to this hypothesis such such as outgoing
 420 longwave radiation (OLR), cloud top pressure (CTP), high cloud fraction (HCF %) and ice to-
 421 tal content (QCF) to better understand the differences between control and nudged experiments.

422 The annual mean difference in HCF and QCF associated with the QBO phase (Fig. 10)
 423 shows that the relationship between high clouds and the QBO is different in nudged versus con-

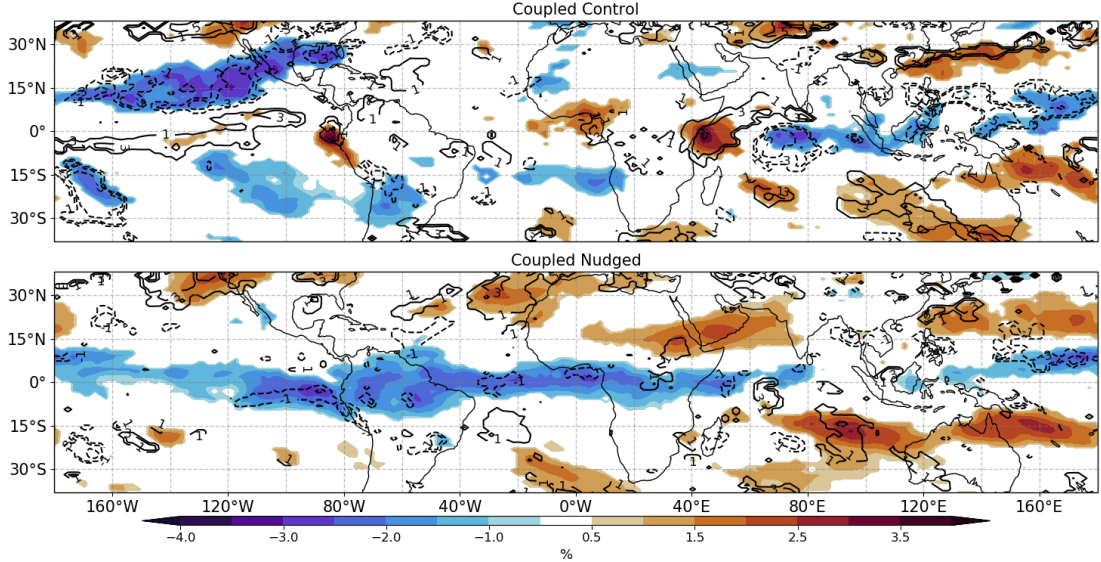


Figure 10. Annual mean differences (QBO W-E during ENSO neutral periods) in high cloud fraction [shading in %] and ice cloud water content [contours in $10^{-2} \text{ kg m}^{-2}$] for Coupled Control and nudged experiments. Only statistically significant (95% confidence level) differences are plotted.

424 control coupled experiments. In the nudged experiments, the QBO signal is much more zonally sym-
 425 metric, characterized by reduced HCF and QCF at equatorial regions under QBOW compared
 426 to QBOE, in agreement with previous observational and modelling studies (Sun et al., 2019; Sakaeda
 427 et al., 2020; Sweeney et al., 2022). In contrast, the differences (W-E) in the free-running control
 428 simulations show a zonally asymmetric response, e.g., with a dipole of positive and negative anoma-
 429 lies in the Indian Ocean.

430 Figure 11 shows the zonal-mean differences (QBO W-E) in convective precipitation and high
 431 cloud diagnostics. First, the control experiments show a dipole response of convective precipi-
 432 tation dipole response in the Indian Ocean, first reported by García-Franco et al. (2022), which
 433 is also observed in OLR, HCF and QCF. In the control experiments, precipitation differences are
 434 strongly anti-correlated with OLR, as expected, and positively correlated with CTP, HCF and
 435 QCF, which illustrates that high cloud occurrence is linked to convective precipitation. However,
 436 the nudged experiments do not exhibit such clear relationships. Instead, the nudged experiments
 437 show a zonally symmetric decrease of HCF under QBOW compared to QBOE. This could sug-
 438 gest that the without dynamical feedbacks, the QBO impact is to decrease HCF at equatorial
 439 latitudes.

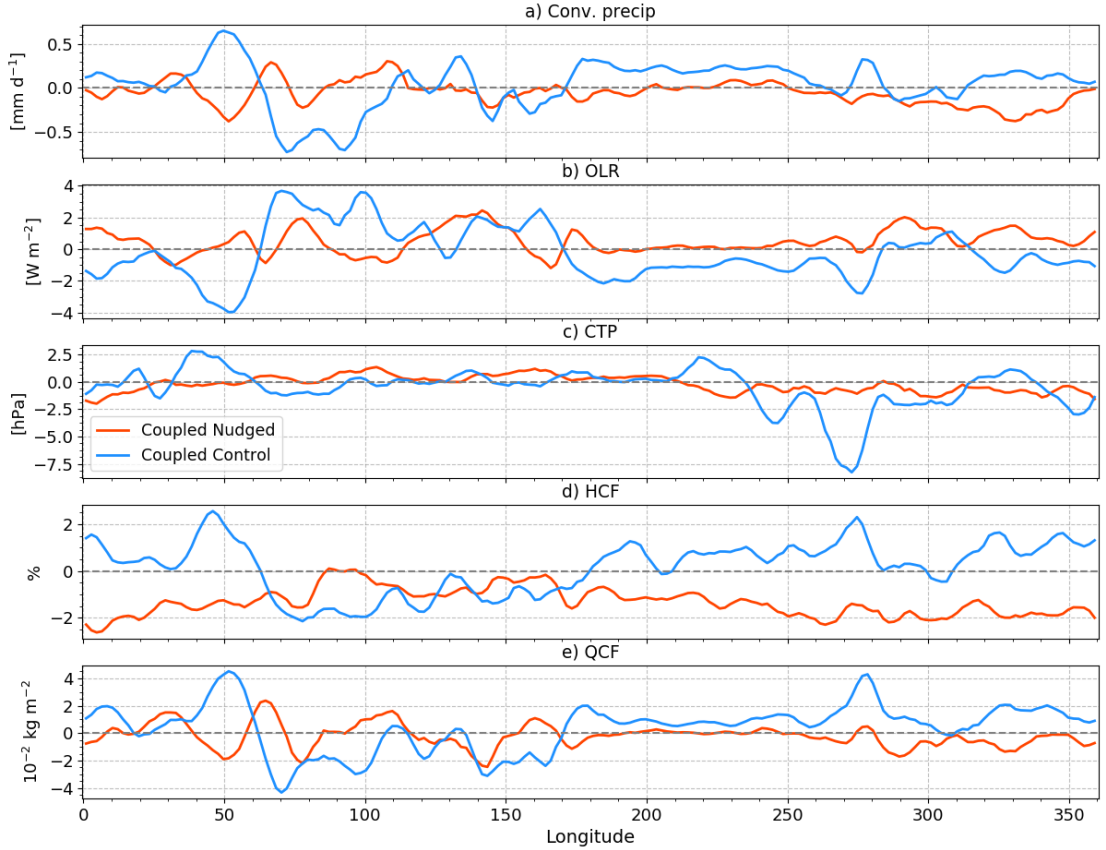


Figure 11. Zonal-mean equatorially averaged [10S-10N] annual-mean differences QBO W-E (during neutral ENSO conditions only) of (a) convective precipitation [mm day^{-1}], (b) OLR [W m^{-2}], (c) cloud top pressure [Pa], (d) high-cloud fraction [%] and (e) ice total content [$10^{-2} \text{ kg m}^{-2}$].

440 In short, this section shows that when the stratosphere is nudged fewer high clouds are found
 441 under QBOW compared to QBOE at equatorial latitudes. In contrast, the control experiments
 442 show zonally asymmetric signals, particularly in the Indian Ocean, which closely follow precip-
 443 itation and OLR anomalies. These results suggest that the interaction between high clouds and
 444 the QBO phase has been modified by the nudging. Despite exhibiting robust zonally symmet-
 445 ric anomalies in HCF, the nudged experiments do not show spatially coherent or robust convec-
 446 tive precipitation differences. This result could suggest that changes to high cloud fraction or ice
 447 content alone are not sufficient for a significant precipitation response.

448 **4 Discussion and conclusions**

449 A set of nudging experiments performed with the MOHC UM was used to investigate three
 450 existing hypotheses that could explain links between the QBO and tropical convection and pre-

451 precipitation. By nudging the zonal wind in the equatorial stratosphere towards ERA5, the UM re-
452 realistically reproduces the observed QBO-related variability in the zonal wind and temperature
453 in the UTLS region. The nudging thus removed the weak QBO amplitude bias in the lower strato-
454 sphere which could modify or weaken QBO tropical surface impacts in GCMs (J. C. K. Lee &
455 Klingaman, 2018; H. Kim, Caron, et al., 2020; Martin et al., 2021a).

456 The analysis of the atmosphere-only experiments has shown that the zonal wind in the equa-
457 torial stratosphere, either nudged or free-running, makes little difference to the simulation of pre-
458 cipitation in the UM with prescribed SSTs as boundary conditions. This result implies that any
459 process that links the QBO to the tropical circulation within the model, such as those diagnosed
460 in García-Franco et al. (2022), requires SSTs to play an active role, either driving the relation-
461 ship or through SST-QBO feedbacks.

462 The role of SST feedbacks for the QBO mechanism was investigated using coupled ocean-
463 atmosphere experiments. In the control experiments, the SSTs over tropical oceans were found
464 to be warmer under QBOW than under QBOE, in agreement with García-Franco et al. (2022).
465 Precipitation patterns in these experiments follow the SSTs with wetter conditions over equa-
466 torial oceans under QBOW compared to QBOE. However, in the nudged ensemble-mean, both
467 SST and precipitation differences were null or close to zero in equatorial regions, meaning that
468 the relationship between the QBO and the tropical surface in the control experiments was muted
469 by the nudging. A closer inspection of other relationships between the QBO and the IOD and
470 ENSO (García-Franco et al., 2022), confirmed that the nudging has notably modified, and in some
471 cases removed, the QBO signal at the tropical surface.

472 One possible explanation for these results is that the simulated QBO-tropical teleconnec-
473 tions are the result of a bottom-up process which is broken when the stratosphere is nudged to-
474 wards a specified state. Since the QBO is tightly coupled to the interaction between convectively
475 triggered waves and the stratospheric mean flow (Baldwin et al., 2001; Y.-H. Kim & Chun, 2015;
476 Geller et al., 2016; Garfinkel et al., 2022), the QBO is modulated by tropical variability such as
477 ENSO events (Schirber, 2015; Serva et al., 2020). Therefore, one could reasonably suspect that
478 the difference between the control and the nudged experiments is simply that waves propagat-
479 ing from the tropical troposphere cannot propagate to the nudged layer in the nudged experi-
480 ments.

481 However, previous studies have found no evidence for an impact from ENSO on to the QBO
482 amplitude and descent rates in the UM (Serva et al., 2020; García-Franco et al., 2022). While

483 tropical waves propagated from the troposphere to the stratosphere are a main control of the QBO
484 characteristics, the impact of upward tropical wave propagation is subtle and does not instan-
485 taneously change the zonal mean wind at 70 hPa (which is our index). This means that the ENSO-
486 QBO relationship in the UM model remains to be explained.

487 Another possibility is that feedbacks that are responsible for the relationships simulated
488 in the control simulations were removed by the nudging. This possibility was investigated using
489 elements from three hypotheses that could explain QBO teleconnections in the tropics: the static
490 stability, the Walker circulation and high cloud feedbacks. The static stability hypothesis sug-
491 gests that the UTLS temperature structure, affected by the QBO on interannual timescales, can
492 modify the strength of convection such that decreased UTLS static stability under QBOE increases
493 convection and precipitation compared to QBOW (Collimore et al., 2003; Liess & Geller, 2012).

494 However, this study shows that the magnitude and sign of the UTLS static stability vari-
495 ability associated with the QBO (Figs. 7 and 8) have no robust relationship with precipitation
496 variability in the deep tropics in the UM. First, the QBO signal in UTLS static stability was found
497 to be zonally symmetric but the QBO signal in precipitation was highly asymmetric. Second, the
498 nudged experiments more than doubled the UTLS static stability variability associated with the
499 QBO, yet the precipitation response to the QBO phase was muted when the nudging was ap-
500 plied. Nevertheless, variability in the UTLS static stability is indeed positively correlated to pre-
501 cipitation variability over tropical oceans (Fig. 8d). The implication from this result is that QBO-
502 related variability in UTLS static stability is not a sufficient process to explain the link between
503 the QBO and tropical convection and other processes amplify or overwhelm the influence of the
504 static stability.

505 A second hypothesis argues that the Walker circulation strength and location is affected
506 by the QBO, which could explain why the precipitation response in the tropics is zonally asym-
507 metric (Hitchman et al., 2021; García-Franco et al., 2022). The coupled experiments showed that
508 the nudging significantly affected the mean-state and variability of the upper branch of the Walker
509 circulation in the Pacific and maritime continent. A weakening of the Walker circulation under
510 QBOW compared to QBOE is diagnosed in observations, the control experiments and other ver-
511 sions of the UM model (Hitchman et al., 2021; García-Franco et al., 2022). However, the QBO-
512 Walker circulation relationship was weakened when the nudging was applied to the model. In
513 fact, the Indian Ocean response even reversed sign relative to the control. One possible expla-
514 nation is that the nudging has overly constrained the upper branch of the Walker circulation, re-

515 moving mean-state biases and, to some extent, the influence from the SSTs on to the 200-100
516 hPa temperature and wind fields (Fig. 9e-f). This result could mean that the Walker circulation
517 plays a role in amplifying local-scale effects of the QBO in a feedback process which was mod-
518 ified by the nudging. used, including cloud fraction and ice cloud content, an Finally, a CRE hy-
519 pothesis has been suggested recently which argues that cirrus clouds play an important role in
520 QBO tropical teleconnections (Sun et al., 2019; Sakaeda et al., 2020; Lin & Emanuel, 2022). This
521 CRE hypothesis could operate at the large-scale, if the QBO modifies the mean-state of clouds
522 in the TTL region (Tseng & Fu, 2017; Sweeney et al., 2022) but also at the convective scale if
523 strength of ascent and vertical advection of water vapour is modified by the QBO (Nie & Sobel,
524 2015; Sakaeda et al., 2020).

525 To investigate this hypothesis, several diagnostics for high clouds were shown to be pos-
526 itively correlated with precipitation changes in the control experiments. In the nudged exper-
527 iments, a robust decreased fraction of high clouds under QBOW compared to QBOE is diagnosed
528 across equatorial regions, which agrees with some observational and modelling evidence (Sun et
529 al., 2019; Sakaeda et al., 2020; Sweeney et al., 2022; Lin & Emanuel, 2022). However, in the nudged
530 experiments differences in high cloud fraction are not related to precipitation or OLR anoma-
531 lies. These results highlight that the simulated QBO teleconnections require tropical stratosphere-
532 troposphere coupling and feedbacks.

533 One possible drawback of the nudging approach employed in this study is that the QBO
534 winds have been nudged to the observations at all longitudes, in contrast to some studies that
535 only nudge the zonal-mean values. While the QBO sets the zonal-mean temperature and wind,
536 the local conditions of clouds, convection and temperature in the tropical UTLS are heavily in-
537 fluenced by feedbacks at the UTLS region involving the horizontal advection of clouds (Lin &
538 Emanuel, 2022), static stability (Nie & Sobel, 2015), or upward wave propagation (Sakaeda et
539 al., 2020; Holt et al., 2022). This means that if the QBO is linked to tropical convection in the
540 UM through the interaction of upward wave propagation and high-clouds, or through large-scale
541 zonal circulations, with the underlying SSTs, our nudging setup was not the appropriate to di-
542 agnose these mechanisms. Based on this hypothesis, the nudging at all longitudes of this study
543 would weaken or even remove the influence of the lower troposphere on the local TTL and mut-
544 ing feedbacks potentially involving large-scale tropical circulations. However, further studies, with
545 different types of nudging or with different models are required to test these hypotheses.

546 **Open Research Section**

547 The reanalysis, observational and CMIP6 data is publicly available (see references in main
548 text). The simulation data will be made publicly available at the time of acceptance.

549 **Acknowledgments**

550 JLGF acknowledges support from an Oxford-Richards Scholarship.

551 **References**

- 552 Adler, R. F., Huffman, G. J., Chang, A., Ferraro, R., Xie, P.-P., Janowiak, J., . . . Nelkin, E.
553 (2003). The version-2 global precipitation climatology project (GPCP) monthly precipita-
554 tion analysis (1979–present). *Journal of hydrometeorology*, *4*(6), 1147–1167.
- 555 Allan, R. P. (2011). Combining satellite data and models to estimate cloud radiative effect
556 at the surface and in the atmosphere. *Meteorological Applications*, *18*(3), 324–333.
- 557 Back, S.-Y., Han, J.-Y., & Son, S.-W. (2020). Modeling evidence of qbo-mjo connection: A
558 case study. *Geophysical Research Letters*, *47*(20), e2020GL089480.
- 559 Baldwin, M., Gray, L., Dunkerton, T., Hamilton, K., Haynes, P., Randel, W., . . . others
560 (2001). The quasi-biennial oscillation. *Reviews of Geophysics*, *39*(2), 179–229.
- 561 Bushell, A. C., Anstey, J. A., Butchart, N., Kawatani, Y., Osprey, S. M., Richter, J. H., . . .
562 Yukimoto, S. (2020). Evaluation of the Quasi-Biennial Oscillation in global climate models
563 for the SPARC QBO-initiative. *Quarterly Journal of the Royal Meteorological Society*,
564 1–31. Retrieved from [https://rmets.onlinelibrary.wiley.com/doi/abs/10.1002/](https://rmets.onlinelibrary.wiley.com/doi/abs/10.1002/qj.3765)
565 [qj.3765](https://doi.org/10.1002/qj.3765) doi: <https://doi.org/10.1002/qj.3765>
- 566 Byrne, M. P., & Zanna, L. (2020). Radiative effects of clouds and water vapor on an axisym-
567 metric monsoon. *Journal of Climate*, *33*(20), 8789–8811.
- 568 Collimore, C. C., Martin, D. W., Hitchman, M. H., Huesmann, A., & Waliser, D. E. (2003).
569 On the relationship between the QBO and tropical deep convection. *Journal of climate*,
570 *16*(15), 2552–2568.
- 571 Davis, S. M., Liang, C. K., & Rosenlof, K. H. (2013). Interannual variability of tropical
572 tropopause layer clouds. *Geophysical Research Letters*, *40*(11), 2862–2866.
- 573 Domeisen, D. I., Garfinkel, C. I., & Butler, A. H. (2019). The teleconnection of El Niño
574 Southern Oscillation to the stratosphere. *Reviews of Geophysics*, *57*(1), 5–47.
- 575 García-Franco, J. L., Gray, L. J., Osprey, S., Chadwick, R., & Martin, Z. (2022). The trop-

- 576 ical route of quasi-biennial oscillation (qbo) teleconnections in a climate model. *Weather*
577 *and Climate Dynamics*, 3(3), 825–844. doi: 10.5194/wcd-3-825-2022
- 578 Garfinkel, C. I., Gerber, E. P., Shamir, O., Rao, J., Jucker, M., White, I., & Paldor, N.
579 (2022). A qbo cookbook: Sensitivity of the quasi-biennial oscillation to resolution, resolved
580 waves, and parameterized gravity waves. *Journal of Advances in Modeling Earth Systems*,
581 14(3), e2021MS002568.
- 582 Garfinkel, C. I., & Hartmann, D. L. (2011). The influence of the quasi-biennial oscillation
583 on the troposphere in winter in a hierarchy of models. Part II: Perpetual winter WACCM
584 runs. *Journal of the Atmospheric Sciences*, 68(9), 2026–2041.
- 585 Geller, M. A., Zhou, T., & Yuan, W. (2016). The qbo, gravity waves forced by tropical con-
586 vection, and enso. *Journal of Geophysical Research: Atmospheres*, 121(15), 8886–8895.
- 587 Giorgetta, M. A., Bengtsson, L., & Arpe, K. (1999). An investigation of QBO signals in the
588 east Asian and Indian monsoon in GCM experiments. *Climate dynamics*, 15(6), 435–450.
- 589 Gray, L., Brown, M., Knight, J., Andrews, M., Lu, H., O’Reilly, C., & Anstey, J. (2020).
590 Forecasting extreme stratospheric polar vortex events. *Nature communications*, 11(1),
591 1–9.
- 592 Gray, L. J., Anstey, J. A., Kawatani, Y., Lu, H., Osprey, S., & Schenzinger, V. (2018).
593 Surface impacts of the Quasi Biennial Oscillation. *Atmospheric Chemistry and Physics*,
594 18(11), 8227–8247. doi: 10.5194/acp-18-8227-2018
- 595 Gray, W. M. (1984). Atlantic seasonal hurricane frequency. Part I: El Niño and 30 mb quasi-
596 biennial oscillation influences. *Monthly Weather Review*, 112(9), 1649–1668.
- 597 Gray, W. M., Sheaffer, J. D., & Knaff, J. A. (1992). Influence of the stratospheric QBO on
598 ENSO variability. *Journal of the Meteorological Society of Japan. Ser. II*, 70(5), 975–995.
- 599 Hartmann, D. L., & Berry, S. E. (2017). The balanced radiative effect of tropical anvil
600 clouds. *Journal of Geophysical Research: Atmospheres*, 122(9), 5003–5020.
- 601 Haynes, P., Hitchcock, P., Hitchman, M., Yoden, S., Hendon, H., Kiladis, G., . . . Simpson,
602 I. (2021). The influence of the stratosphere on the tropical troposphere. *Journal of the*
603 *Meteorological Society of Japan. Ser. II*.
- 604 Hendon, H. H., & Abhik, S. (2018). Differences in vertical structure of the madden-julian
605 oscillation associated with the quasi-biennial oscillation. *Geophysical Research Letters*,
606 45(9), 4419–4428.
- 607 Hersbach, H., Bell, B., Berrisford, P., Hirahara, S., Horányi, A., Muñoz-Sabater, J., . . .
608 Thépaut, J.-N. (2020). The ERA5 global reanalysis. *Quarterly Journal of the Royal*

- 609 *Meteorological Society*, 146(730), 1999–2049. doi: 10.1002/qj.3803
- 610 Hitchman, M. H., Yoden, S., Haynes, P. H., Kumar, V., & Tegtmeier, S. (2021). An ob-
611 servational history of the direct influence of the stratospheric quasi-biennial oscillation on
612 the tropical and subtropical upper troposphere and lower stratosphere. *Journal of the*
613 *Meteorological Society of Japan. Ser. II.*
- 614 Holt, L. A., Lott, F., Garcia, R. R., Kiladis, G. N., Cheng, Y.-M., Anstey, J. A., ... others
615 (2022). An evaluation of tropical waves and wave forcing of the qbo in the qboi models.
616 *Quarterly Journal of the Royal Meteorological Society*, 148(744), 1541–1567.
- 617 Hu, Z.-Z., Huang, B., Kinter, J. L., Wu, Z., & Kumar, A. (2012). Connection of the strato-
618 spheric QBO with global atmospheric general circulation and tropical SST. Part II: inter-
619 decadal variations. *Climate dynamics*, 38(1), 25–43.
- 620 Kennedy, J. J., Rayner, N., Atkinson, C., & Killick, R. (2019). An ensemble data set of sea
621 surface temperature change from 1850: The met office hadley centre hadsst. 4.0. 0.0 data
622 set. *Journal of Geophysical Research: Atmospheres*, 124(14), 7719–7763.
- 623 Kim, H., Caron, J. M., Richter, J. H., & Simpson, I. R. (2020). The lack of QBO-MJO
624 Connection in CMIP6 Models. *Geophysical Research Letters*, 47(11), e2020GL087295.
625 (e2020GL087295 2020GL087295) doi: 10.1029/2020GL087295
- 626 Kim, H., Son, S.-W., & Yoo, C. (2020). Qbo modulation of the mjo-related precipitation in
627 east asia. *Journal of Geophysical Research: Atmospheres*, 125(4), e2019JD031929.
- 628 Kim, Y.-H., & Chun, H.-Y. (2015). Contributions of equatorial wave modes and parameter-
629 ized gravity waves to the tropical qbo in hadgem2. *Journal of Geophysical Research: At-*
630 *mospheres*, 120(3), 1065–1090.
- 631 Lee, J. C. K., & Klingaman, N. P. (2018). The effect of the quasi-biennial oscillation on
632 the Madden–Julian oscillation in the Met Office Unified Model Global Ocean Mixed Layer
633 configuration. *Atmospheric Science Letters*, 19(5), e816. doi: 10.1002/asl.816
- 634 Lee, J.-H., Kang, M.-J., & Chun, H.-Y. (2019). Differences in the tropical convective activi-
635 ties at the opposite phases of the quasi-biennial oscillation. *Asia-Pacific Journal of Atmo-*
636 *spheric Sciences*, 55(3), 317–336.
- 637 Liess, S., & Geller, M. A. (2012). On the relationship between qbo and distribution of tropi-
638 cal deep convection. *Journal of Geophysical Research: Atmospheres*, 117(D3).
- 639 Lim, Y., & Son, S.-W. (2022). Qbo wind influence on mjo-induced temperature anomalies in
640 the upper troposphere and lower stratosphere in an idealized model. *Journal of the Atmo-*
641 *spheric Sciences.*

- 642 Lin, J., & Emanuel, K. (2022). Stratospheric modulation of the mjo through cirrus cloud
643 feedbacks. *Journal of the Atmospheric Sciences*.
- 644 Martin, Z., Orbe, C., Wang, S., & Sobel, A. (2021a). The MJO–QBO Relationship in a
645 GCM with Stratospheric Nudging. *Journal of Climate*, *34*(11), 4603–4624.
- 646 Martin, Z., Sobel, A., Butler, A., & Wang, S. (2021c). Variability in qbo temperature
647 anomalies on annual and decadal time scales. *Journal of Climate*, *34*(2), 589–605.
- 648 Martin, Z., Son, S.-W., Butler, A., Hendon, H., Kim, H., Sobel, A., . . . Zhang, C. (2021b).
649 The influence of the quasi-biennial oscillation on the madden–julian oscillation. *Nature Re-*
650 *views Earth & Environment*, 1–13.
- 651 Martin, Z., Wang, S., Nie, J., & Sobel, A. (2019, 02). The Impact of the QBO on MJO Con-
652 vection in Cloud-Resolving Simulations. *Journal of the Atmospheric Sciences*, *76*(3), 669-
653 688.
- 654 Menary, M. B., Kuhlbrodt, T., Ridley, J., Andrews, M. B., Dimdore-Miles, O. B., Deshayes,
655 J., . . . Xavier, P. (2018). Preindustrial control simulations with HadGEM3-GC3. 1 for
656 CMIP6. *Journal of Advances in Modeling Earth Systems*, *10*(12), 3049–3075.
- 657 Nie, J., & Sobel, A. H. (2015). Responses of tropical deep convection to the QBO: Cloud-
658 resolving simulations. *Journal of the Atmospheric Sciences*, *72*(9), 3625–3638.
- 659 Rao, J., Garfinkel, C. I., & White, I. P. (2020). How does the quasi-biennial oscillation affect
660 the boreal winter tropospheric circulation in cmip5/6 models? *Journal of Climate*, *33*(20),
661 8975–8996.
- 662 Richter, J. H., Anstey, J. A., Butchart, N., Kawatani, Y., Meehl, G. A., Osprey, S., & Simp-
663 son, I. R. (2020). Progress in simulating the Quasi-Biennial Oscillation in CMIP models.
664 *Journal of Geophysical Research: Atmospheres*, *125*(8), e2019JD032362. (e2019JD032362
665 10.1029/2019JD032362)
- 666 Sakaeda, N., Dias, J., & Kiladis, G. N. (2020). The unique characteristics and potential
667 mechanisms of the mjo-qbo relationship. *Journal of Geophysical Research: Atmospheres*,
668 *125*(17), e2020JD033196.
- 669 Schenzinger, V., Osprey, S., Gray, L., & Butchart, N. (2017). Defining metrics of the Quasi-
670 Biennial oscillation in global climate models. *Geoscientific Model Development*, *10*(6).
- 671 Schirber, S. (2015). Influence of ENSO on the QBO: Results from an ensemble of idealized
672 simulations. *Journal of Geophysical Research: Atmospheres*, *120*(3), 1109–1122.
- 673 Serva, F., Anstey, J. A., Bushell, A. C., Butchart, N., Cagnazzo, C., Gray, L., . . . Simpson,
674 I. R. (2022). The impact of the QBO on the region of the tropical tropopause in QBOi

- 675 models: present-day simulations. *Quarterly Journal of the Royal Meteorological Society*,
676 *148*(745), 1945-1964. doi: <https://doi.org/10.1002/qj.4287>
- 677 Serva, F., Cagnazzo, C., Christiansen, B., & Yang, S. (2020). The influence of enso events on
678 the stratospheric qbo in a multi-model ensemble. *Climate Dynamics*, *54*(3), 2561–2575.
- 679 Son, S.-W., Lim, Y., Yoo, C., Hendon, H. H., & Kim, J. (2017). Stratospheric control of the
680 Madden–Julian oscillation. *Journal of Climate*, *30*(6), 1909–1922.
- 681 Storkey, D., Blaker, A. T., Mathiot, P., Megann, A., Aksenov, Y., Blockley, E. W., ... others
682 (2018). UK Global Ocean GO6 and GO7: A traceable hierarchy of model resolutions.
683 *Geoscientific Model Development*, *11*(8), 3187–3213.
- 684 Sun, L., Wang, H., & Liu, F. (2019). Combined effect of the qbo and enso on the mjo. *Atmo-*
685 *spheric and Oceanic Science Letters*, *12*(3), 170–176.
- 686 Sweeney, A. J., Fu, Q., Pahlavan, H. A., & Haynes, P. (2022, aug). Seasonality of the QBO
687 impact on equatorial clouds. *ESSOAR*. Retrieved from [https://doi.org/10.1002/](https://doi.org/10.1002/2Fessoar.10512278.1)
688 [2Fessoar.10512278.1](https://doi.org/10.1002/2Fessoar.10512278.1) doi: 10.1002/essoar.10512278.1
- 689 Tegtmeier, S., Anstey, J., Davis, S., Ivanciu, I., Jia, Y., McPhee, D., & Pilch Kedzierski, R.
690 (2020). Zonal Asymmetry of the QBO Temperature Signal in the Tropical Tropopause
691 Region. *Geophysical Research Letters*, *47*(24), e2020GL089533. (e2020GL089533
692 2020GL089533) doi: <https://doi.org/10.1029/2020GL089533>
- 693 Telford, P., Braesicke, P., Morgenstern, O., & Pyle, J. (2008). Description and assessment of
694 a nudged version of the new dynamics unified model. *Atmospheric Chemistry and Physics*,
695 *8*(6), 1701–1712.
- 696 Trenberth, K. E. (1997). The definition of el nino. *Bulletin of the American Meteorological*
697 *Society*, *78*(12), 2771–2778.
- 698 Tseng, H.-H., & Fu, Q. (2017). Temperature control of the variability of tropical tropopause
699 layer cirrus clouds. *Journal of Geophysical Research: Atmospheres*, *122*(20), 11–062.
- 700 Walters, D., Boutle, I., Brooks, M., Melvin, T., Stratton, R., Vosper, S., ... Xavier, P.
701 (2019). The Met Office Unified Model global atmosphere 7.0/7.1 and JULES global land
702 7.0 configurations. *Geoscientific Model Development*, *12*(5), 1909–1963.
- 703 Yoo, C., & Son, S.-W. (2016). Modulation of the boreal wintertime madden-julian oscillation
704 by the stratospheric quasi-biennial oscillation. *Geophysical Research Letters*, *43*(3), 1392–
705 1398.

1 **Understanding the mechanisms for tropical surface impacts**
2 **of the quasi-biennial oscillation (QBO)**

3 **Jorge L. García-Franco^{1,2}, Lesley J. Gray^{1,3}, Scott Osprey^{1,3}, Robin Chadwick^{4,5} and**
4 **Jonathan Lin²**

5 ¹Atmospheric, Oceanic and Planetary Physics, University of Oxford

6 ²Lamont-Doherty Earth Observatory, Columbia University, NY

7 ³National Centre for Atmospheric Science, Oxford, United Kingdom

8 ⁴Met Office Hadley Centre, UK

9 ⁵Global Systems Institute, Department of Mathematics, University of Exeter, Exeter, UK

10 **Key Points:**

- 11 • Nudging the zonal wind in the equatorial stratosphere affects tropical convection variabil-
12 ity only in coupled ocean-atmosphere simulations.
- 13 • The impact of the quasi-biennial oscillation (QBO) on upper-level static stability is not
14 sufficient to influence tropical precipitation.
- 15 • Interactions between upward wave propagation and upper-level clouds is the likely mech-
16 anism of QBO tropical teleconnections.

Corresponding author: Lesley J. Gray, lesley.gray@physics.ox.ac.uk

Abstract

This study evaluates the main hypotheses to explain a coupling between the quasi-biennial oscillation (QBO) in the tropical stratosphere and the tropical troposphere and surface. The impact of the QBO on tropical convection and precipitation is investigated through nudging experiments using the UK Met Office Hadley Centre Unified Model (UM). The model control simulations show robust links between the internally generated QBO and tropical precipitation and circulation. The model zonal wind in the tropical stratosphere was nudged above 90 hPa in atmosphere-only and coupled ocean-atmosphere configurations. The simulation of convection and precipitation in the atmosphere-only simulations is not statistically significantly different between the experiments with and without nudging, which may indicate that SST-convection coupling is needed for any QBO influence on the tropical lower troposphere and surface. In the coupled experiments, the precipitation and SST relationships with the QBO phase disappear when nudging is applied. Evidence from the nudging experiments shows that the QBO influence over lower stratospheric static stability is not sufficient to produce tropical surface impacts. The nudging also reduced the influence of the lower troposphere to the upper branch of the Walker circulation, irrespective of the QBO, indicating that the upper troposphere has been slightly decoupled from the surface by the nudging. These results suggest that nudging all grid-points might mute relevant feedback processes, including high cloud radiative effects and wave mean flow interactions, occurring at the tropopause level.

Plain Language Summary

The interaction between the stratosphere and the troposphere is well known to produce surface impacts in the extratropics. However, whether stratosphere-troposphere interactions affect the surface in the tropics associated with the variability of the stratospheric quasi-biennial oscillation (QBO) is yet to be determined because the observational record is too short and tropical tropospheric variability masks any potential signal of the stratosphere. In this paper, we examine hypotheses that suggest the stratospheric quasi-biennial oscillation can affect tropical deep convection to the extent of influencing tropical surface precipitation variability through targeted model experiments which prescribe the equatorial stratosphere towards observations. Our results indicate that prescribing the zonal wind in the stratosphere remove links between surface precipitation and the QBO. The weight of the evidence in our findings suggest that the impact of the QBO on the static stability at the interface of the QBO and tropical convection is not enough

to produce significant effects over tropical convection and precipitation but high clouds in the tropics could play a bigger role than previously thought.

1 Introduction

The stratospheric quasi-biennial oscillation (QBO) has been linked to tropical deep convection for several decades (W. M. Gray, 1984; Giorgetta et al., 1999; Collimore et al., 2003; Liess & Geller, 2012). Observations show that the magnitude and location of tropical precipitation and several cloud properties are statistically related to the QBO phase (Liess & Geller, 2012; Tseng & Fu, 2017; L. J. Gray et al., 2018; H. Kim, Son, & Yoo, 2020; Hitchman et al., 2021; García-Franco et al., 2022; Sweeney et al., 2022). However, the extent to which the tropical troposphere and stratosphere are coupled, as well as the mechanisms that connect these two layers, remain a matter of debate (Haynes et al., 2021; Hitchman et al., 2021; Martin et al., 2021b).

Firstly, the relatively short observational record which limits our ability to detect any robust response of tropical precipitation to the QBO phase (Hu et al., 2012; García-Franco et al., 2022). The strong influence of El Niño-Southern Oscillation (ENSO) over tropical variability on interannual timescales is also a limiting factor for the attribution of anomalies in the tropics to the QBO (Liess & Geller, 2012; L. J. Gray et al., 2018; J.-H. Lee et al., 2019), especially because the ENSO-QBO relationship appears to have changed between 1960-1985 and 1985-2020 (Domeisen et al., 2019; García-Franco et al., 2022).

Secondly, there is no clear understanding of how the QBO could modulate tropical deep convection. Several hypotheses have been suggested to potentially explain a coupling of the QBO and the tropical troposphere including static stability (e.g. Nie & Sobel, 2015; Haynes et al., 2021), vertical wind shear (e.g. W. M. Gray et al., 1992), a QBO-Walker circulation feedback (Collimore et al., 2003; Hu et al., 2012; Hitchman et al., 2021; García-Franco et al., 2022) and cloud feedback hypotheses (Sakaeda et al., 2020). However, there is no clear understanding which of these hypotheses, if any, is the primary mechanism for a downward impact from the QBO on tropical convection.

The static stability hypothesis suggests that the meridional circulation driven by the descending QBO shear impacts the static stability in the region of the upper troposphere-lower stratosphere (UTLS; W. M. Gray et al., 1992; Giorgetta et al., 1999; Collimore et al., 2003; Liess & Geller, 2012; Nie & Sobel, 2015; Back et al., 2020). These studies argue that decreased UTLS static stability is found under the easterly phase (QBOE) compared to the westerly phase (QBOW),

79 leading to enhanced convection under QBOE (Collimore et al., 2003) which could explain, e.g.,
80 the stronger convection associated with the Madden-Julian Oscillation (MJO) under QBOE con-
81 ditions (Yoo & Son, 2016; Son et al., 2017; Hendon & Abhik, 2018; Back et al., 2020).

82 Observational and modelling results indicate that the QBO impact in the tropics is not zon-
83 ally symmetric (Collimore et al., 2003; Liess & Geller, 2012; García-Franco et al., 2022). For this
84 reason, several studies have suggested an interaction between the QBO and the Walker circula-
85 tion (Liess & Geller, 2012; Hu et al., 2012; Hitchman et al., 2021). Observations show that the
86 Walker circulation was weaker under QBOW compared to QBOE in the period of 1979-2021 (Hitch-
87 man et al., 2021; García-Franco et al., 2022) but the causal direction of this relationship remains
88 to be well understood.

89 A different hypothesis, however, suggests that cloud-radiative effects (CREs) associated with
90 the variability of tropical upper-level cirrus clouds explain the QBO-MJO link (Sun et al., 2019;
91 Sakaeda et al., 2020; Martin et al., 2021b; Lim & Son, 2022; Lin & Emanuel, 2022). Given the
92 importance of cirrus clouds for the radiative budget in the tropics due to their longwave CRE
93 (Allan, 2011; Hartmann & Berry, 2017) and the role of the QBO modulating variability of clouds
94 in the tropical tropopause layer (TTL) on interannual timescales (Liess & Geller, 2012; Davis et
95 al., 2013; Tseng & Fu, 2017; Tegtmeier et al., 2020; Sweeney et al., 2022), the QBO could rea-
96 sonably affect convection through CRE at different scales. Evidence for this hypothesis has shown
97 that more high-cloud coverage associated with the MJO is observed during QBOE compared to
98 QBOW (Sun et al., 2019; Sakaeda et al., 2020), suggesting that CREs associated with the QBO
99 could be a relevant mechanism for QBO tropical teleconnections. In short, despite the growing
100 number of hypotheses that explain a potential link between the QBO and tropical convective fea-
101 tures, a clear mechanism remains to be determined.

102 Since observations and theory have not successfully identified the mechanism for QBO tropi-
103 cal teleconnections, several studies have turned to numerical models such as cloud-resolving mod-
104 els (Nie & Sobel, 2015; Martin et al., 2019; Back et al., 2020) and General Circulation Models
105 (GCMs; J. C. K. Lee & Klingaman, 2018; H. Kim, Caron, et al., 2020; Serva et al., 2022) to iden-
106 tify pathways of stratospheric-tropospheric coupling. Although GCMs are more comprehensive,
107 stratospheric and tropospheric biases have hindered the potential use of these models to tackle
108 this problem because GCMs underestimate the amplitude of the QBO in the lowermost strato-
109 sphere (Fig. S1 and J. C. K. Lee & Klingaman, 2018; H. Kim, Caron, et al., 2020; Martin et al.,
110 2021a). For this reason, the variability of the UTLS static stability associated with the QBO is

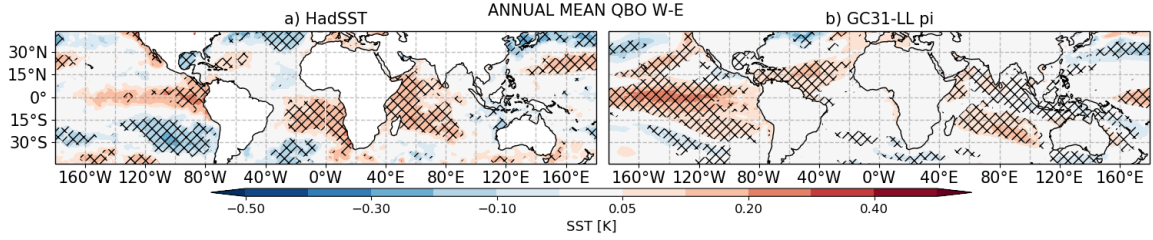


Figure 1. Annual mean SST [K] QBO W-E differences in (a) HadSST dataset and (b) the pre-industrial control simulation of the UM GC31-LL pi. Hatching denotes significance to the 95% confidence level.

111 lower than observed in models (Schenzinger et al., 2017; J. C. K. Lee & Klingaman, 2018; Bushell
 112 et al., 2020; Richter et al., 2020; Rao et al., 2020).

113 This weak amplitude bias in the QBO has been hypothesized to explain why some observed
 114 teleconnections, including the MJO-QBO relationship, are not diagnosed in GCMs (J. C. K. Lee
 115 & Klingaman, 2018; H. Kim, Caron, et al., 2020; Martin et al., 2021a). Due to these biases, sev-
 116 eral studies have performed or suggested experiments in which the model stratosphere is relaxed
 117 towards an observed or idealized state of the stratosphere, also known as nudging (e.g. Garfinkel
 118 & Hartmann, 2011; J. C. K. Lee & Klingaman, 2018; Richter et al., 2020; Martin et al., 2021a).
 119 The nudging technique can remove biases, identify causal pathways and test specific hypothe-
 120 ses to understand mechanisms (L. Gray et al., 2020; Haynes et al., 2021).

121 This study aims to understand QBO tropical teleconnections by addressing the issue of QBO
 122 model biases using relaxation experiments of the Met Office Hadley Centre (MOHC) Unified Model
 123 (UM). The UM is a state-of-the-art GCM that is able to simulate an internally generated QBO
 124 that is reasonably similar to observations, except for the weak amplitude bias in the lower strato-
 125 sphere (Richter et al., 2020). In addition, nudging has previously been successfully applied in this
 126 model (Telford et al., 2008; L. Gray et al., 2020). The UM exhibits robust connections between
 127 the tropical troposphere associated with the QBO, which are described in García-Franco et al.
 128 (2022), including a sea-surface temperature (SST) signal (see Figure 1) that is similar to the ob-
 129 served record and El Niño events occur more frequently under QBOW compared to QBOE.

130 The main purpose of this study is to evaluate the effect of nudging on the representation
 131 of the QBO surface impacts in the tropics. The results of these experiments will be used to crit-
 132 ically examine existing hypotheses suggested to explain QBO-convection links: the static stabil-

133 ity mechanism and QBO-Walker circulation relationships, and the role of CREs. The remain-
134 der of this paper is presented as follows. Section 2 describes the nudging experiments, as well as
135 the observations, CMIP6 and reanalysis datasets used to compare the experimental results. Sec-
136 tion 3 presents the results of the experiments. The final section presents a discussion and con-
137 clusions arising from this study.

138 2 Methods and data

139 2.1 Observations and reanalysis

140 Observational data of precipitation and SSTs are used in this study. The Global Precip-
141 itation Climatology Project (GPCP) v2.3 (Adler et al., 2003) dataset is used for precipitation
142 analyses and the HadSST v4.0 (Kennedy et al., 2019) for SST. For the remaining diagnostics,
143 including the zonal wind and convective precipitation we use the reanalysis ERA5 from the Eu-
144 ropean Centre for Medium-Range Weather Forecasts (ECMWF) (Hersbach et al., 2020) down-
145 loaded at the $0.75 \times 0.75^\circ$ resolution from <https://cds.climate.copernicus.eu/cdsapp>. In all
146 cases the data cover the period 1979-2021.

147 2.2 The Met Office Unified Model

148 The MOHC UM uses a seamless approach modelling framework that allows the setup of
149 simulations using various configurations; for example, various horizontal resolutions maintain-
150 ing the same parametrizations and dynamical core (Walters et al., 2019). In addition to the main
151 experimental design for nudging used in this study, which is explained in detail in the following
152 section, the CMIP6 preindustrial control experiment from the MOHC model HadGEM3 is used
153 for comparison. The preindustrial control experiments use constant external forcing integrated
154 for 500 years (Menary et al., 2018). In this study we use results from the HadGEM3 GC3.1 N96
155 (GC31-LL) experiment.

156 2.3 Nudging scheme

157 Nudging refers to the relaxation of a model variable towards a specified state, which can
158 be taken from reanalysis, observations or idealized states (L. Gray et al., 2020; Martin et al., 2021a).
159 In the UM setup, three variables can be nudged: air temperature (T) and the zonal (u) and merid-
160 ional (v) components of the wind; in this study we use ERA5 as the nudging data. The relax-
161 ation is applied at each grid-point, in contrast to other studies (e.g. Martin et al., 2021a) that

162 employ a spectral model and apply the relaxation only to the zonal-mean component. Specif-
 163 ically, the UM uses a Newtonian relaxation technique (Telford et al., 2008; L. Gray et al., 2020)
 164 which sets the field to be nudged (F) at each time-step through the following equation:

$$\Delta F = G\Delta t(F_{ndg} - F_{model}), \quad (1)$$

165 where ΔF is the discrete change of F at each time-step, G is the relaxation parameter, Δt is the
 166 time-step size, F_{ndg} is the value of the field from the nudging data and F_{model} is the model value
 167 of the field at the last time-step (Telford et al., 2008).

168 The relaxation parameter G sets the strength of the relaxation and is linked with the re-
 169 laxation timescale (τ) by $G = 1/\tau$. Previous studies (Telford et al., 2008; L. Gray et al., 2020)
 170 have shown that a 6-h relaxation time-scale is sufficient to constrain the stratosphere in the model
 171 and so the same parameter was used for the simulations of this chapter ($G = \frac{1}{6} \text{ h}^{-1}$).

172 Furthermore, the nudging can be performed between specified vertical levels and in selected
 173 latitude/longitude regions with *tapering*, which refers to a linear interpolation between the max-
 174 imum G and zero nudging ($G = 0$). The chosen experimental design relaxes only the zonal wind
 175 (u) at all longitudes in the latitude band of 20°S-20°N, with a 10° tapering, at the model lev-
 176 els corresponding to 90 hPa to 4 hPa, with a vertical tapering of 4 levels, which means that full
 177 nudging was in effect only at 10°S-10°N from 70 hPa to 10 hPa. The experimental setup aims
 178 to reasonably simulate the observed variability of the zonal wind leaving the meridional compo-
 179 nent of the wind and the temperature to respond freely within the model.

180 2.4 Experimental design

181 The configuration of the UM model used for the nudging experiments is GC3.1 (version 11.4),
 182 which is the same configuration as the CMIP6 experiments (Walters et al., 2019). All the exper-
 183 iments, AMIP and coupled, are set up using a present-day climate configuration where all ex-
 184 ternal forcings are set constant to those of the year 2000. The atmospheric horizontal resolution
 185 is N96 (1.875°x1.25°) for our experiments. A summary of all the experiments is given in Table
 186 1.

187 The atmosphere-only (AMIP) experiments were conducted for 32 years (1981-2012) using
 188 prescribed SST and sea-ice boundary conditions for the period 1981-2012, using the data pro-
 189 vided as part of the CMIP6 AMIP forcing setup. Three sets of AMIP experiments were run: Con-

Table 1. Experimental setup indicating the model configuration, the period, number of ensemble members (Ens.) and relaxation details.

Name	Configuration	Period	Ens.	Nudging
AMIP	Atmosphere-only	1981-2012	3	ERA5.
AMIP-Control	Atmosphere-only	1981-2012	3	No nudging
AMIP-Shifted	Atmosphere-only	1981-2012	3	ERA5 Relaxation shifted -1 year.
Coupled Nudged	Coupled ocean-atmosphere	1981-2015	6	ERA5.
Coupled Control	Coupled ocean-atmosphere	1981-2015	6	No nudging

190 trol, Nudged and Shifted. In the control experiment, the model stratosphere was free to evolve.
 191 In the Nudged experiment, the equatorial zonal wind was nudged, as described in the previous
 192 section, with the nudging wind data matching the corresponding SST data.

193 In addition, we performed another type of atmosphere-only experiment, the Shifted exper-
 194 iment. In the normal AMIP Nudged experiment, the SST driving data corresponds to the same
 195 year as the nudged zonal wind in the equatorial stratosphere. In the Shifted experiment, the nudg-
 196 ing data was shifted with a -1 year lag from the SSTs, e.g., the model year 1997 was run using
 197 1997 SSTs but zonal winds in the stratosphere corresponding to 1996. An alternative approach
 198 would be to *shuffle* the SSTs so that each year is run with randomly selected SSTs. However,
 199 since we are performing multi-year simulations shuffling has associated issues of how to join the
 200 randomly-selected SSTs at the year-boundary to form a coherent multi-year SST time-series. To
 201 avoid this issue we decided to simply shift the zonal wind nudging data by one year so the QBO
 202 phase and SSTs were not aligned.

203 For the coupled ocean-atmosphere experiments, a control and a nudged ensemble of 6 mem-
 204 bers were run for 35 years (1981-2015 model years). The coupled experiments use an oceanic res-
 205 olution of 0.25° (ORCA025) using the NEMO model (Storkey et al., 2018). Each ensemble mem-
 206 ber was initialized from different ocean/atmosphere initial conditions, in order to decrease the

207 role that internal variability may have on these simulations by averaging out the ensemble. Specif-
 208 ically, the coupled ocean-atmosphere configuration was initialized using oceanic conditions from
 209 a 100-yr simulation of the same model configuration that were found 10 years apart from each
 210 other.

211 2.5 Indices and methods

212 ENSO is measured through the standard Oceanic Niño Index, i.e., the time-series of area-
 213 averaged SSTs in the Niño 3.4 region (hereafter EN3.4 Trenberth, 1997) and a 5-month running
 214 mean using a 0.5 K threshold to define positive or negative events. The QBO index is defined
 215 using the equatorially-averaged [10S-10N] zonal winds at the 70 hPa level and a $\pm 2 \text{ m s}^{-1}$ thresh-
 216 old to define W and E phases. A measure of the zonal gradient of convective activity in the In-
 217 dian Ocean is used as a proxy of the Indian Ocean Dipole (IOD), as in García-Franco et al. (2022).
 218 Composite and regression analysis are used to evaluate the differences amongst experiments, as
 219 in García-Franco et al. (2022). Statistical significance in observations and individual ensemble
 220 members is diagnosed using a bootstrapping method with replacement, whereas for all ensemble-
 221 mean differences, given their relative larger sample size, standard two-sided t-tests are used.

222 3 Results

223 Figure 2 demonstrates that nudging increases the UTLS temperature and zonal wind vari-
 224 ability associated with the QBO. The comparison of the QBO W-E difference between the nudged
 225 experiments, ERA5, the 500-yr CMIP6 GC31-LL simulation, and the control experiments shows
 226 that the nudged experiments closely resemble the results from ERA5 whereas the control exper-
 227 iments exhibit a much weaker signal. In the tropical UTLS region, the nudged experiments show
 228 a wider and stronger QBO signal than the control experiments which demonstrates that these
 229 experiments are suitable to explore the processes that relate the QBO with the tropical surface.
 230 The control-nudged difference plots (Fig. S2) illustrate that the warm anomalies near the equa-
 231 torial tropopause between 70-90 hPa are up to 1.5 K larger in the nudged experiments.

232 Since the nudging technique has removed the weak QBO amplitude bias in the lower strato-
 233 sphere, we now analyse tropical teleconnections in these experiments. First, results from the atmosphere-
 234 only experiments are analysed, followed by the analysis of the coupled experiments. The final
 235 section investigates the mechanisms that could explain the differences between nudged and con-
 236 trol experiments.

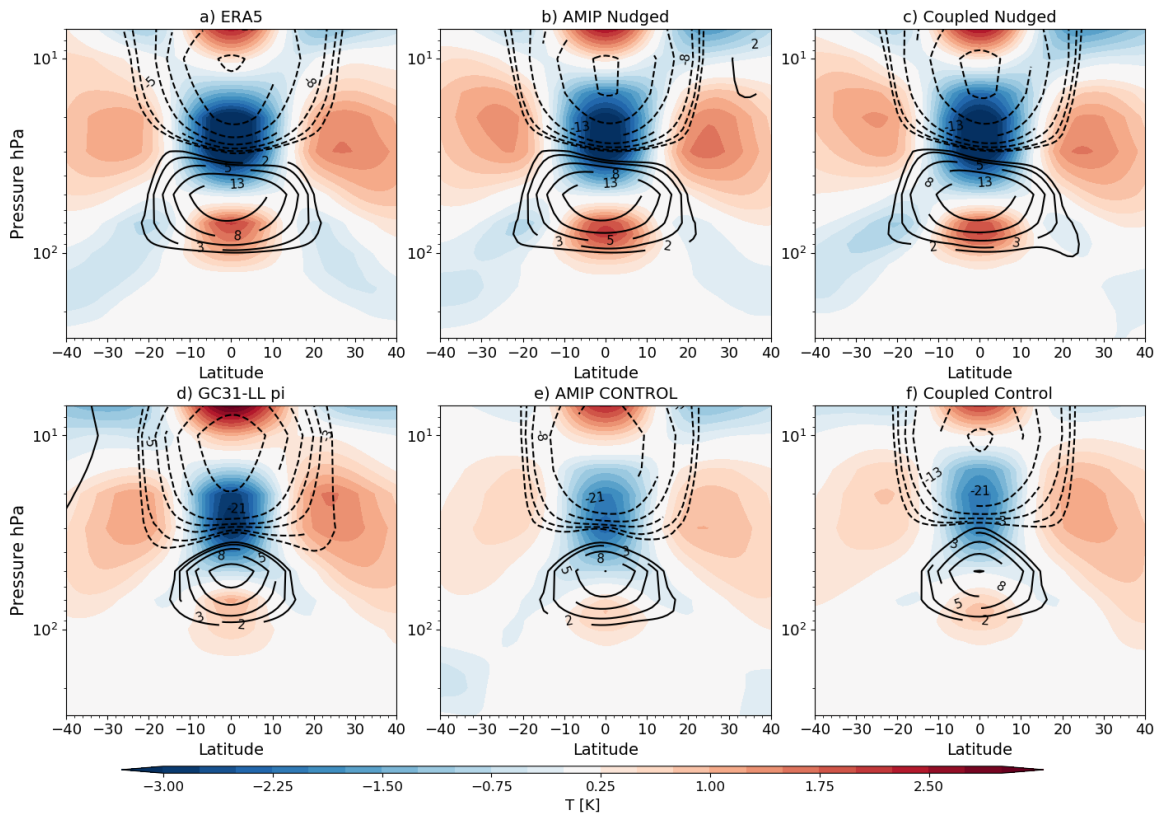


Figure 2. Latitude-height plot of the zonal-mean temperature (shading) zonal wind (contours in m s^{-1}) QBO W-E differences in (a) ERA5, the nudged simulations in (b) AMIP and (c) coupled configurations and (d) GC31 N96-pi from CMIP6, the control simulations with no nudging in an (e) AMIP and (f) coupled configurations

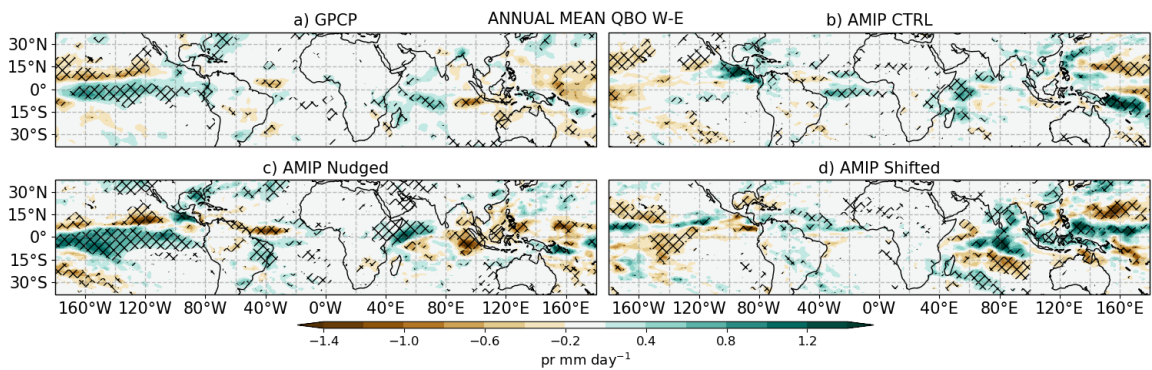


Figure 3. Annual-mean precipitation response (QBO W-E) in (a) GPCP, and atmosphere-only experiments: (b) AMIP CTRL, (c) AMIP Nudged and (d) AMIP Shifted.

238 This section shows the results of the atmosphere-only experiments: AMIP Nudged, AMIP
 239 Control and AMIP Shifted (in which the imposed winds have been shifted by a year so there is
 240 an out-of-phase relaxation of the winds with respect to the SSTs), compared to observations (1981-
 241 2012). The annual-mean difference of precipitation between QBOW and E phases from the three
 242 experiments are compared with GPCP differences in Fig. 3. The AMIP Nudged ensemble-mean
 243 matches closely the results of GPCP, characterised by an El Niño pattern in the Pacific Ocean,
 244 a weaker Atlantic ITCZ and a zonal gradient of precipitation in the Indian Ocean during QBOW
 245 compared to QBOE.

246 In contrast, the differences in the AMIP Control and the AMIP Shifted experiments show
 247 little similarity to the observed response, a similar result is found for seasonal-mean composite
 248 differences (see e.g. Fig S3). The fact that the QBO response is different in the three types of
 249 AMIP experiments suggests that the underlying SSTs, and not the QBO winds, are responsible
 250 for these differences. However, it may still be the case that tropical convection is sensitive to the
 251 QBO phase in these simulations and this effect is hidden by the strong effect of SST forcing.

252 Time-series of multiple diagnostics averaged at equatorial latitudes and in the EN3.4 re-
 253 gions are shown in Figure 4. The tropical mean outgoing longwave radiation (OLR) and precip-
 254 itation is not significantly affected by the nudging, suggesting that convective activity is inde-
 255 pendent from the state of the QBO at 70 hPa. The correlation coefficients of precipitation and
 256 OLR with respect to observations (a-b) are indistinguishable between experiments, both for the
 257 tropics-wide (a, c) and for the EN3.4 region (b, d).

258 The timeseries of the equatorial zonal mean zonal wind at 70 hPa (U_{70} ; Fig. 4e) shows a
 259 correlation between ERA5 and the Nudged experiment, as expected. In contrast, the correlation
 260 of ERA5 with AMIP CTRL is virtually zero, because the ensemble-mean zonal wind of the CTRL
 261 collapses to near zero values. The Shifted experiment shows a negative and high correlation (0.65)
 262 with ERA5, which is not surprising, since the SSTs have been shifted by one year i.e. approx-
 263 imately half a QBO cycle.

264 The timeseries of the near-tropopause temperature (T_{100} ; Fig. 4g-h) shows that the Nudged
 265 ensemble is correlated with ERA5 in the tropical mean. This correlation increases for the EN3.4
 266 region in all the experiments such that the three simulations are well correlated with ERA5, al-
 267 though the Shifted experiment shows the lowest correlation. These results suggest the near-tropopause
 268 temperature is controlled by the QBO in the zonal-mean but by local SSTs at regional scales.
 269 In short, this section shows that in atmosphere-only experiments the nudging produces the ex-

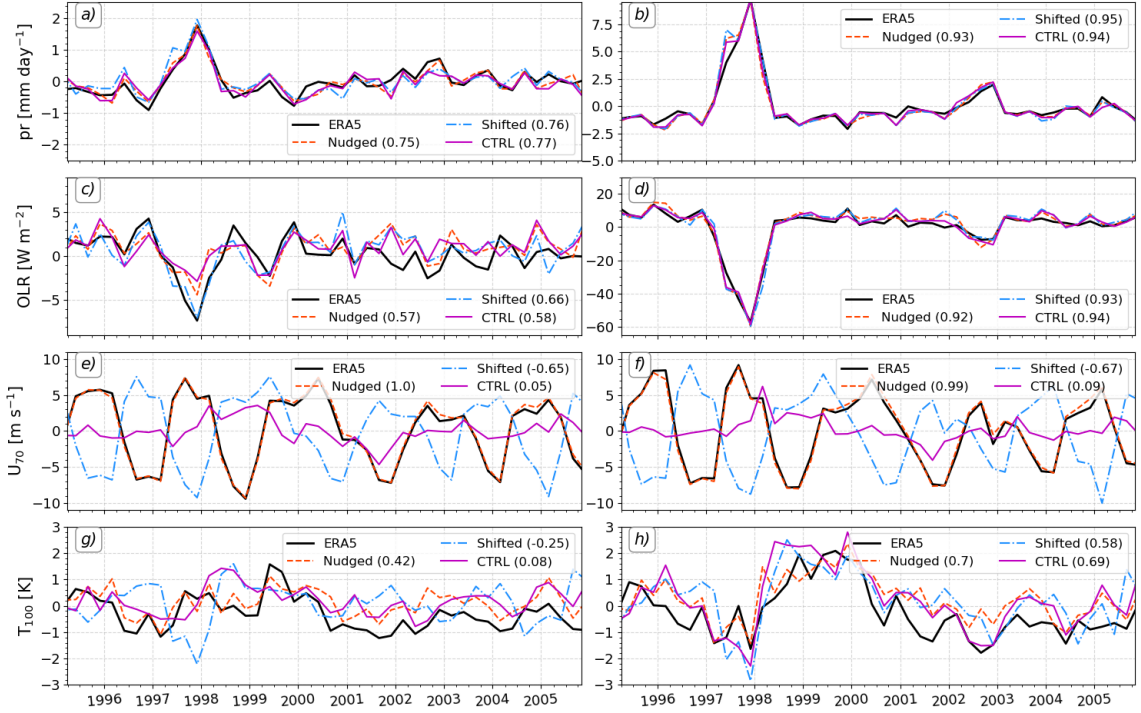


Figure 4. Time-series in the atmosphere-only experiments of (a, b) precipitation, (c, d) outgoing longwave radiation (OLR), (e, f) zonal wind at 70 hPa (U_{70}) and (g, h) air temperature at 100 hPa. The timeseries are shown for quantities averaged over the (left) zonal-mean equatorial $[5^{\circ}\text{S}-5^{\circ}\text{N}]$ and (right) EN3.4 regions. For each AMIP experiment the Pearson correlation coefficient between the experiment and ERA5 is shown in the legend. Note that the model year refers to the SST years as described in section 22.4.

270 expected impacts in U_{70} and the zonal-mean T_{100} , however, the nudging appears to have no made
 271 impact on the simulation of precipitation and OLR.

272 3.2 Coupled experiments

273 This section analyses the coupled ocean-atmosphere experiments, labelled as the Coupled
 274 Nudged and the Coupled Control simulations, which consist of 6 ensemble members (see section
 275 22.4). The SST response is first examined through the annual mean QBO W-E ensemble-mean
 276 difference in tropical SSTs of the coupled control experiments (Fig 5a-b) which compares rea-
 277 sonably well with the results from HadSST and GC3 LL-pi (Fig. 1). This response is character-
 278 ized by warmer SSTs (+0.2-0.3K) during QBOW than during QBOE in the deep tropics and gener-
 279 ally cooler subtropical oceans. However, for the Coupled Nudged ensemble-mean, the tropi-

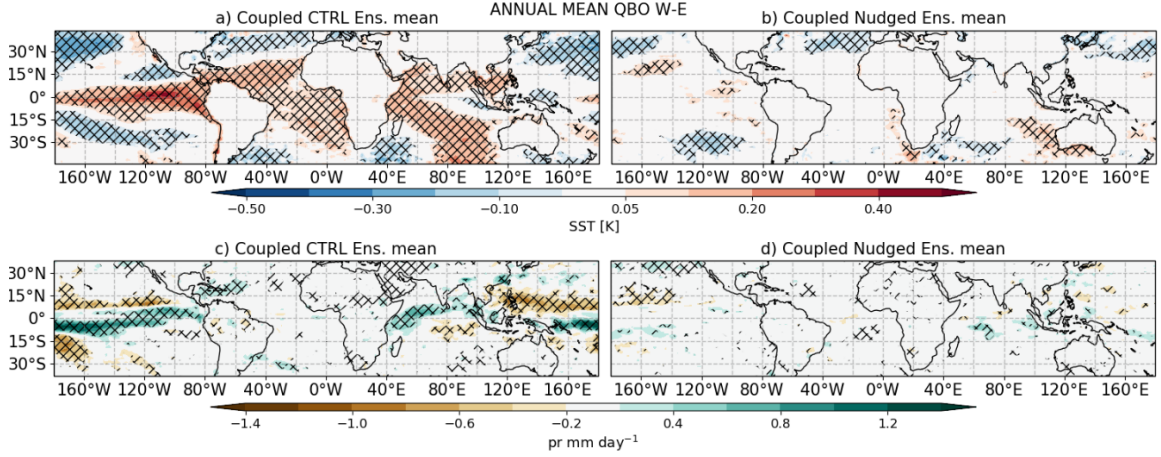


Figure 5. As in Fig. 1 but for results of the (a, c) Coupled Control and (b, d) Coupled Nudged ensemble-mean (a, b) SST [K] and (c, d) precipitation [mm day^{-1}].

280 cal response is essentially zero, although some sparse regions showing slight cooling (W-E) can
 281 be observed in the subtropics. This means that the nudging has affected the physical mechanism
 282 behind the robust statistical relationship between the tropical SSTs and the QBO phase in the
 283 UM (García-Franco et al., 2022).

284 The QBO W-E differences in each of the 6 ensemble members in the Control and Nudged
 285 experiments (Fig. S4) show that the weak response in the ensemble-mean of the nudging exper-
 286 iments is the result of very different responses from each ensemble member. These individual re-
 287 sponses cancel out to a large extent. In contrast, most of the control ensemble members exhibit
 288 a warming signal in the equatorial oceans, leading to the statistically significant response seen
 289 in the ensemble-mean.

290 The precipitation response (Fig. 5c-d) follows closely the SST patterns. The robust rela-
 291 tionship between the QBO and tropical precipitation in the UK UM (García-Franco et al., 2022)
 292 is also observed in the Control experiment characterized by shifts of the ITCZ in the Pacific and
 293 Atlantic sectors and a wetter western Indian Ocean. This relationship is, however, removed, when
 294 the nudging is applied as the nudged ensemble-mean is virtually zero across the tropics, which
 295 is also due to the cancelling effect of different responses in individual ensemble members (Fig.
 296 S5).

297 One key result from García-Franco et al. (2022) was a robust relationship between the QBO
 298 and the IOD during boreal fall. Figure 6 shows that this relationship is also robust in the Con-

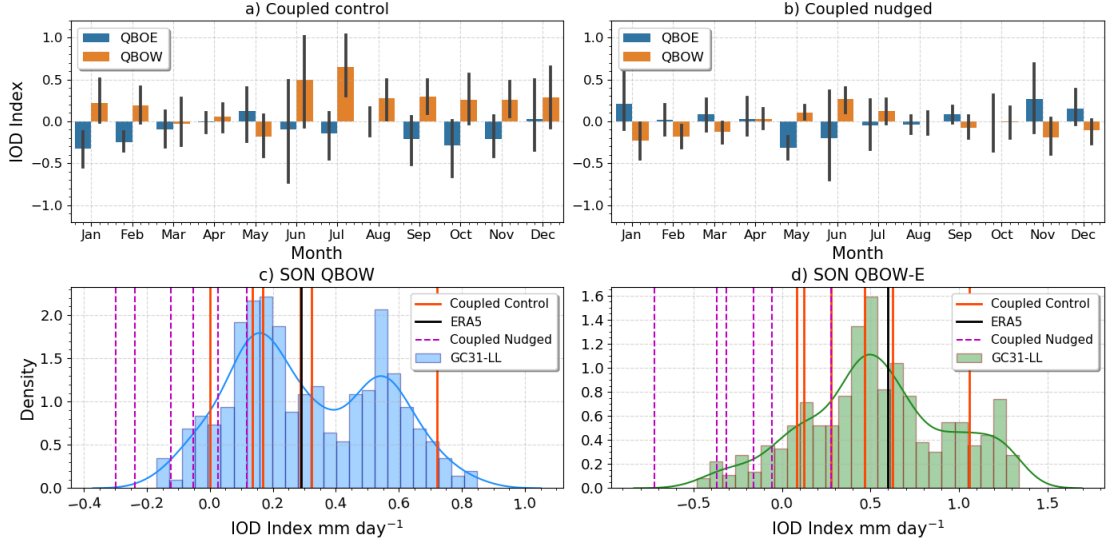


Figure 6. (a, b) Monthly-mean convective precipitation IOD index [mm day⁻¹] in coupled (a) control and (b) nudged ensemble-means separated by QBO phase; the error bars indicate ensemble spread. (c, d) Probability density functions (PDFs) of the IOD convective precipitation index for (c) the mean SON during QBOW months and (d) the SON difference between QBO W-E. The PDF is obtained by bootstrapping the 500 yr simulation of the GC31-LL 42-yr periods and obtaining the averages and differences in each sub-sample. The mean values for the Coupled Control and Nudged experiments, as well as for ERA5 are shown as vertical lines.

299 control experiments of this configuration but not in the Coupled Nudged experiments. A probabil-
 300 ity density function (PDF) of QBO W-E in the IOD index was constructed using 35-yr chunks
 301 of the pre-industrial control experiment GC31-LL to sample internal variability within the model.
 302 The difference in the IOD index per QBO phase for individual ensemble members from the Control
 303 and Nudged experiments is plotted together with the GC31-LL PDF (Fig. 6c-d) to exam-
 304 ine the likelihood that the results from the Nudged experiments happen by chance.

305 The results in Fig. 6c-d strongly suggest that the influence on the IOD is removed when
 306 nudging is applied given that some ensemble Nudged members show differences that are outside
 307 of the 99% range of the PDF whereas all the Control experiments show results that fall close to
 308 the median of the GC31-LL PDF. The results for the EN3.4 index are very similar (Supplemen-
 309 tary Fig. S6) confirming the ENSO-QBO relationship has been removed by the nudging.

310 This section shows that the coupled control experiments in our configuration broadly re-
 311 produce those of García-Franco et al. (2022), i.e., warmer SSTs and wetter conditions in the deep

312 tropics in QBOW compared to QBOE as well as statistical links between the QBO and ENSO
 313 and the IOD. However, nudging has significantly affected the relationships between the QBO and
 314 the tropical troposphere. Several plausible explanations, including the possibility that the sta-
 315 tistical relationships diagnosed by García-Franco et al. (2022) are simply due to an upward ef-
 316 fect from the troposphere to the stratosphere, are discussed in the final section. The following
 317 section evaluates three hypotheses using these experiments.

318 **3.3 Mechanisms**

319 The main mechanisms suggested by the literature to possibly explain a role for the QBO
 320 in modulating aspects of tropical convection are the static stability, QBO-Walker circulation and
 321 high-cloud effects. This section aims to evaluate these hypotheses through a comparison of the
 322 coupled nudged and Control experiments.

323 **3.3.1 The static stability hypothesis**

324 The effect of the QBO over the tropical UTLS temperature structure has been well doc-
 325 umented (Tegtmeier et al., 2020; Martin et al., 2021c) and is, arguably, the most frequently sug-
 326 gested mechanism that relates tropical convection variability to the QBO (Collimore et al., 2003;
 327 Liess & Geller, 2012; Hu et al., 2012; Nie & Sobel, 2015; J. C. K. Lee & Klingaman, 2018; Hitch-
 328 man et al., 2021). The UTLS static stability is defined here by the temperature difference (ΔT)
 329 between 150 and 70 hPa, so that negative values indicate decreased stability. Other definitions
 330 of ΔT such as the temperature difference between 250 hPa and 70 hPa, as well as using the 100
 331 hPa temperature field as a proxy yield similar results to our definition.

332 Figure 7 shows the QBO (W-E) signal in ΔT and convective precipitation. The spatial dis-
 333 tribution of the ΔT differences is relatively zonally symmetric, although for ERA5 and the nudged
 334 experiments ΔT maximizes in the Eastern Pacific. The magnitude of the QBO-related variabil-
 335 ity in ΔT is doubled by the nudging in the deep tropics compared to the control experiments,
 336 however the precipitation response is not increased in the nudged experiment. The precipitation
 337 response to the QBO in models and observations is, firstly, not zonally symmetric and secondly,
 338 not collocated with the largest influence of the QBO signal on the static stability differences.

339 The relationship between the UTLS static stability and tropical precipitation is investigated
 340 in more detail in Figure 8. This figure shows several scatter plots of the spatial and temporal re-
 341 lationship between the static stability and precipitation in both reanalysis and our model sim-

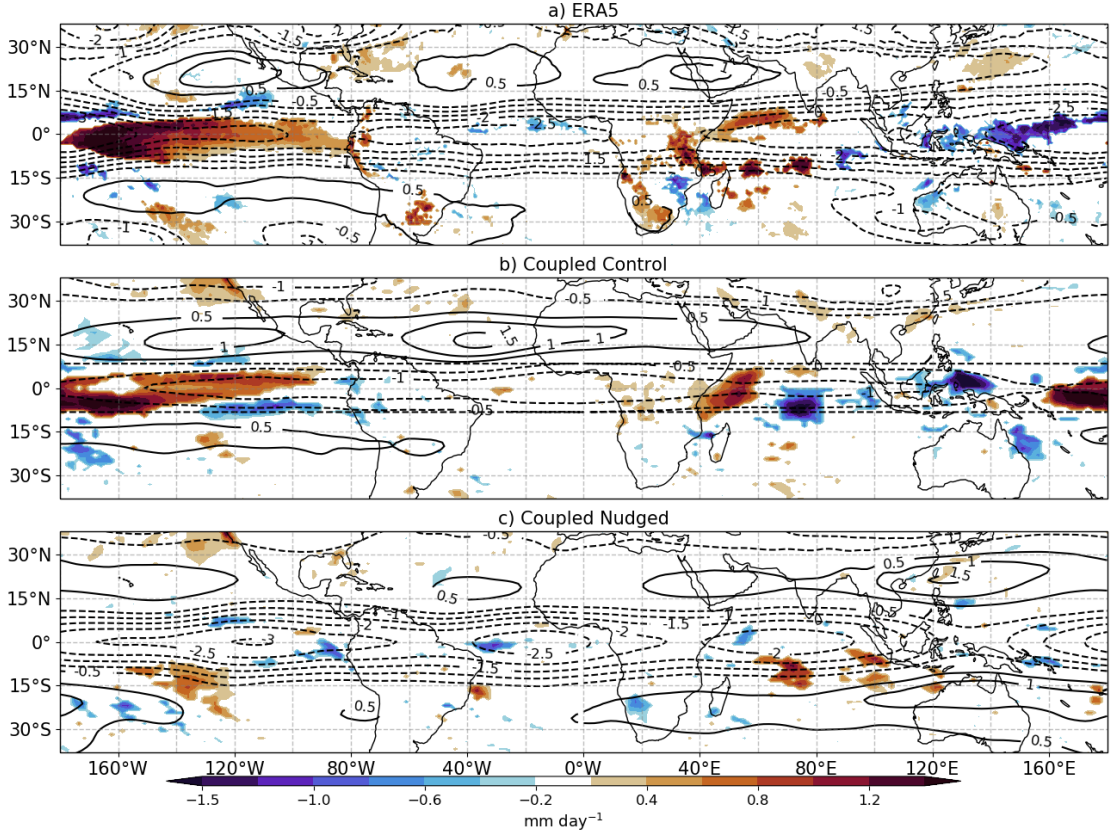


Figure 7. Convective precipitation (shading) and UTLS static stability (ΔT contours in [K]) DJF composite differences (QBO W-E) in (a) ERA5 and the ensemble-mean Coupled (b) Control and (c) Nudged experiments. Only statistically significant differences to the 95% confidence level are plotted.

342 ulations. First, Figure 8a shows the scatter plot of the monthly-averaged ΔT versus Δpr in the
 343 equatorial Western Pacific; such that each points represents a month in ERA5. Therefore, this
 344 figure shows that these two variables have a very weak temporal correlation. In other words, in
 345 ERA5, the temporal variability of the UTLS static stability is not related to precipitation vari-
 346 ability in the West Pacific warm pool. The sign of the correlation coefficient (weak in any case)
 347 reverses between QBOW months and QBOE months. Similar results are found for the simula-
 348 tions (not shown).

349 Next, Figure 8b shows a scatterplot of the annual mean QBO W-E differences of ΔT ver-
 350 sus Δpr at each grid-point in the Coupled nudged and Coupled Control experiments. The mag-
 351 nitude of the negative ΔT differences is higher in the nudged experiments than in the control whereas
 352 the spread of the precipitation differences is higher in the control. This figure illustrates that the
 353 nudging increases the spread of the ΔT differences but not of precipitation. Moreover, in the con-

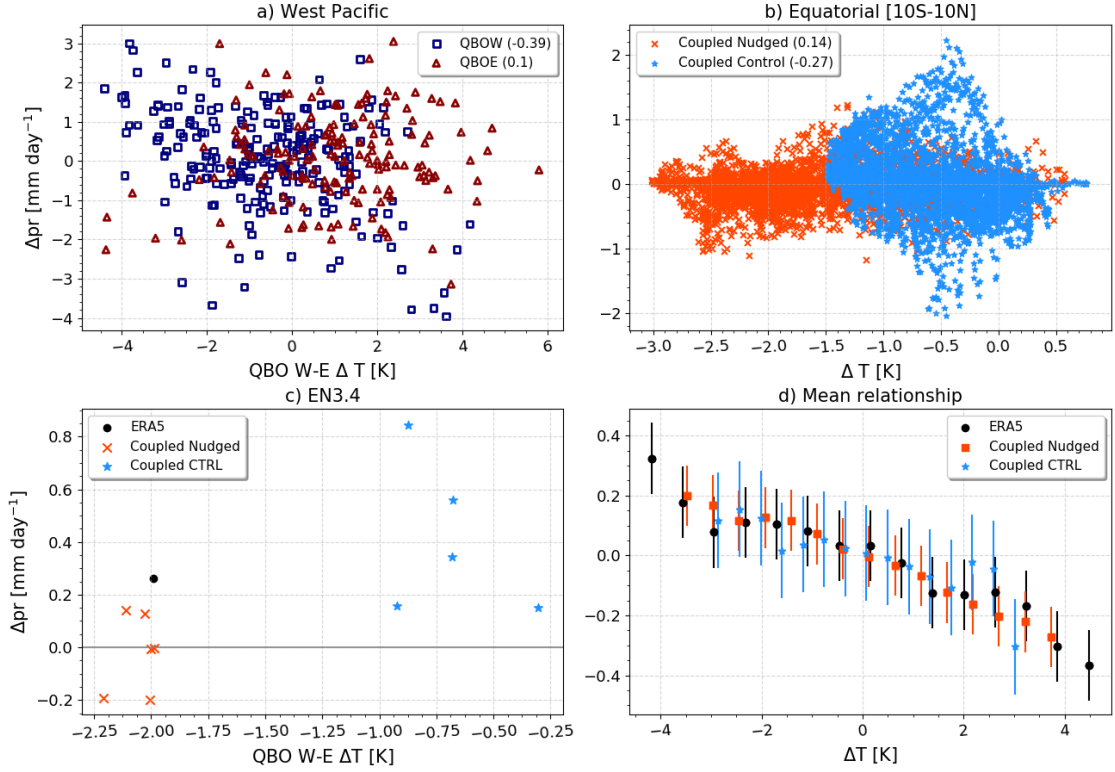


Figure 8. a) Scatter plot of deseasonalized convective precipitation [Δpr mm d⁻¹] versus UTLS static stability [ΔT K] anomalies for the western equatorial Pacific [0-10N,120-160E] in ERA5. Each data-point represents a month in the 1979-2021 period. b) As in a) but for the DJF ensemble-mean QBO W-E differences in the equatorial latitudes [10S-10N] in the simulations, so each dot represents a grid-point. c) Scatter plot of the annual-mean QBO W-E differences in Δpr versus ΔT in the EN3.4 region for each ensemble member of the simulations and ERA5. d) Mean relationship of Δpr versus ΔT computed by binning ΔT in all the grid-points at all times and computing the corresponding mean Δpr .

354 trol experiments, both positive and negative precipitation differences are found for similar ranges
 355 of ΔT differences. The existence of both positive and negative differences in Δpr for similar val-
 356 ues of ΔT in the control indicates that there is no unique longitudinally coherent or zonally sym-
 357 metric impact of the QBO. Additionally, this plot suggests that the magnitude of the precipi-
 358 tation differences are not explained by ΔT differences.

359 Then, Figure 8c shows how annual mean QBO W-E differences in ΔT are related to Δpr
 360 in the Niño3.4 region for each ensemble member of the control and nudged experiments. All the
 361 coupled control ensembles show a positive precipitation difference (W-E) of up to 0.85 mm day⁻¹,
 362 even though the static stability difference (W-E) is half as strong compared to the nudged ex-

363 periments. The nudged ensemble members, in contrast, simulate both positive and negative pre-
 364 cipitation responses close to 0, indicative of no statistical relationship between ENSO and the
 365 QBO in these experiments.

366 Finally, Figure 8d analyses the average relationship between ΔT and Δpr . In this plot, all
 367 the monthly-mean anomalies of convective precipitation and absolute values of ΔT have been
 368 composited using all the grid-points at equatorial latitudes [10°S-10°N] for all the months in each
 369 simulation. This procedure pairs Δpr and ΔT taken at the same time and space coordinates. From
 370 this composite, the average Δpr anomalies were computed for equally-separated bins of ΔT (start-
 371 ing at the 1th percentile and up to the 99th percentile). In this plot, the variability of ΔT is not
 372 necessarily associated with the QBO but the purpose of this plot is investigate whether precip-
 373 itation anomalies are related to the upper-level temperature structure more generally.

374 Therefore, Figure 8d shows the average precipitation anomaly for each ΔT bin. The mean
 375 relationship across the different datasets appears to be of a weak negative relationship which be-
 376 comes significant for high absolute values of ΔT characterized by higher static stability associ-
 377 ated with less precipitation and decreased UTLS static stability associated with more precipi-
 378 tation. This result would support the main assumption of the static stability mechanism, i.e.,
 379 that decreased upper level static stability associated with the QBO leads to more precipitation.
 380 This Figure also confirms that the nudging has increased ΔT variability but the nudging has only
 381 increased precipitation variability only for negative ΔT values.

382 The implication from these results is that nudging has increased ΔT variability and indeed
 383 UTLS static stability is linked to precipitation, however, the time-mean composite differences,
 384 shown in the previous section, suggest that these local-scale ΔT impacts are not enough to sim-
 385 ulate a time-mean significant signal on surface precipitation. In other words, this section presents
 386 evidence that in the UM and ERA5, QBO-related changes to static stability are not a sufficient
 387 factor to modulate tropical convection.

388 ***3.3.2 The Walker circulation***

389 Several studies have suggested a link between the QBO and the Walker circulation (Liess
 390 & Geller, 2012; Hitchman et al., 2021; García-Franco et al., 2022): specifically, in the UM the
 391 Walker circulation is weaker under QBOW than under QBOE. Figure 9 shows the impact of nudg-
 392 ing on the mean state and QBO-ENSO related variability of the Walker circulation. The biases
 393 in the mean-state of the Walker circulation are large in the control experiment, with differences

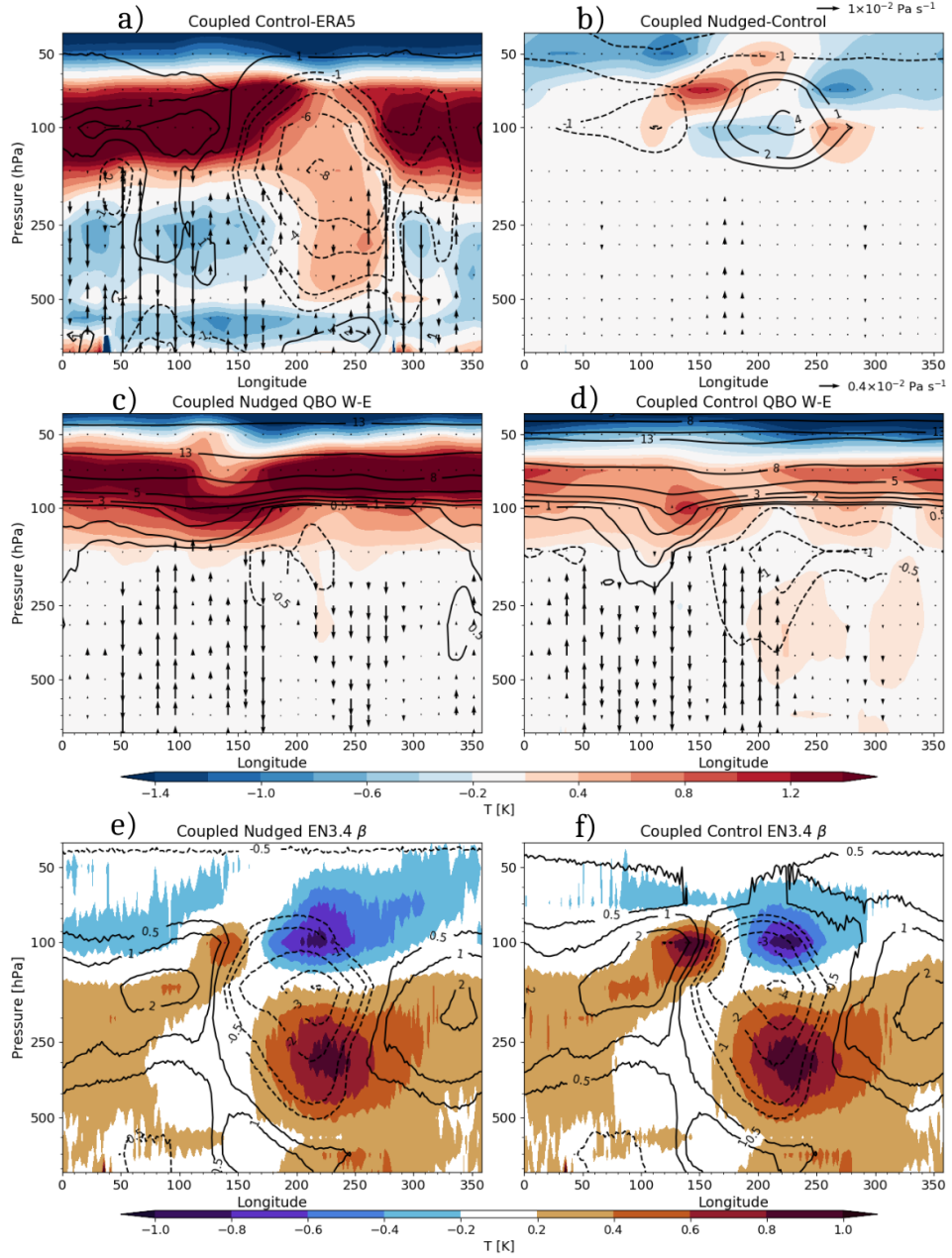


Figure 9. (a) Mean biases, diagnosed as differences between control ensemble-mean and ERA5, in the Walker circulation, (equatorial averages [10S-10N]) diagnosed from the zonal mean temperature (K in shading), zonal wind (contours in m s^{-1}) and vertical velocity (vectors in Pa s^{-1}). (b) shows the differences between nudged and Control coupled experiments. (c-d) show the QBO W-E differences for the (c) nudged and (d) Control ensemble-mean. (c-d) is as in (a-b) except that the (c-d) vector key is different than for (a-b). (e-f) show the results of the regression coefficients (β) between the zonal wind (contours) and the air temperature (shading) fields with the EN3.4 index.

394 of up to 6 m s^{-1} and 1.5 K compared to ERA5 (Fig. 9a). However, nudging improves some of
 395 the zonal wind biases (b), especially in the Pacific Ocean, while also producing an impact on UTLS
 396 temperature biases ($\approx 0.5 \text{ K}$).

397 The QBO-related Walker circulation variability appears to be affected by the nudging. In
 398 the upper troposphere, the QBO impact on the zonal wind and vertical velocities is different for
 399 nudged and control experiments (c versus d). This difference is more obvious in the Indian Ocean
 400 sector where the control experiments suggest that the W-E response is characterized by anoma-
 401 lous ascent in the western sector and descent in the eastern sector, yet the nudged response is
 402 the opposite.

403 Regression analysis was used to investigate the interaction of ENSO, the QBO and the Walker
 404 circulation, as in García-Franco et al. (2022). Figures 9e-f suggest that not only are the mean-
 405 state and the QBO relationships affected but the linear relationship between ENSO and the up-
 406 per branch of the Walker circulation is weakened when the nudging was applied (see e.g. 150E
 407 at 100 hPa where the temperature signal is twice as large in the control experiment). Note, how-
 408 ever, that the lower tropospheric ENSO signal remains unchanged.

409 These results suggest that the effect from ENSO on to the UTLS temperature has been weak-
 410 ened by the nudging which suggests that the nudging may have overly constrained the upper-
 411 branch of the Walker circulation. Feedback processes between convection and the UTLS tem-
 412 perature may have been reduced in strength and the temperature field, constrained through ther-
 413 mal wind balance, which are perhaps related to the nature of the nudging conducted in this study
 414 (see section 4 for a more detailed discussion on this possibility).

415 **3.3.3 The CRE hypothesis**

416 High cirrus CREs are a key aspect of tropical climate (Hartmann & Berry, 2017; Byrne &
 417 Zanna, 2020) such that recent studies have suggested mechanisms through which CREs explain
 418 the observed MJO-QBO connection (Sun et al., 2019; Lin & Emanuel, 2022; Lim & Son, 2022).
 419 This section uses model diagnostics that are relevant to this hypothesis such such as outgoing
 420 longwave radiation (OLR), cloud top pressure (CTP), high cloud fraction (HCF %) and ice to-
 421 tal content (QCF) to better understand the differences between control and nudged experiments.

422 The annual mean difference in HCF and QCF associated with the QBO phase (Fig. 10)
 423 shows that the relationship between high clouds and the QBO is different in nudged versus con-

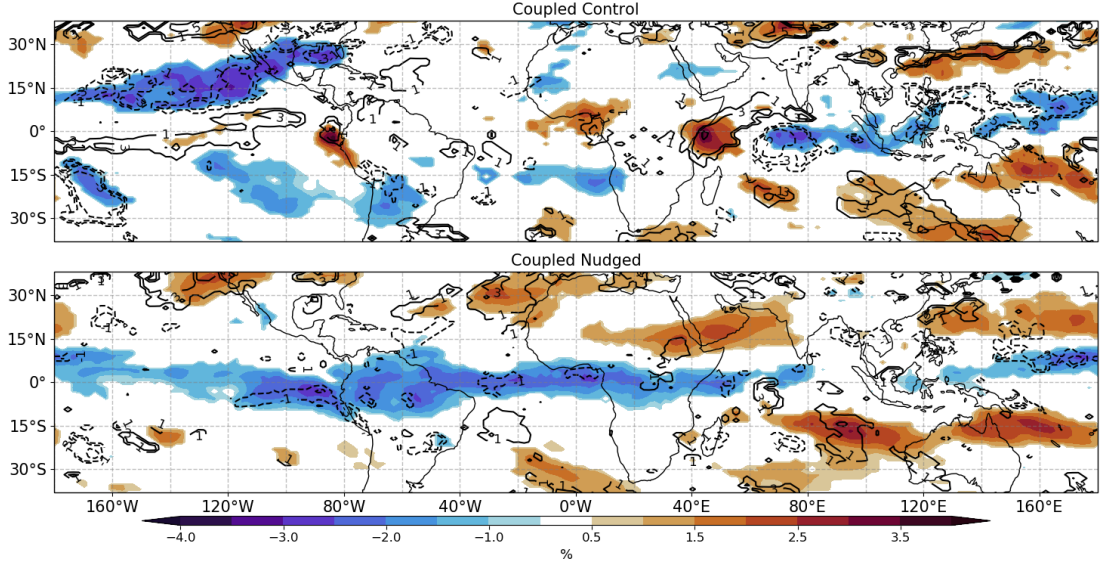


Figure 10. Annual mean differences (QBO W-E during ENSO neutral periods) in high cloud fraction [shading in %] and ice cloud water content [contours in 10^{-2} kg m $^{-2}$] for Coupled Control and nudged experiments. Only statistically significant (95% confidence level) differences are plotted.

424 control coupled experiments. In the nudged experiments, the QBO signal is much more zonally sym-
 425 metric, characterized by reduced HCF and QCF at equatorial regions under QBOW compared
 426 to QBOE, in agreement with previous observational and modelling studies (Sun et al., 2019; Sakaeda
 427 et al., 2020; Sweeney et al., 2022). In contrast, the differences (W-E) in the free-running control
 428 simulations show a zonally asymmetric response, e.g., with a dipole of positive and negative anoma-
 429 lies in the Indian Ocean.

430 Figure 11 shows the zonal-mean differences (QBO W-E) in convective precipitation and high
 431 cloud diagnostics. First, the control experiments show a dipole response of convective precipi-
 432 tation dipole response in the Indian Ocean, first reported by García-Franco et al. (2022), which
 433 is also observed in OLR, HCF and QCF. In the control experiments, precipitation differences are
 434 strongly anti-correlated with OLR, as expected, and positively correlated with CTP, HCF and
 435 QCF, which illustrates that high cloud occurrence is linked to convective precipitation. However,
 436 the nudged experiments do not exhibit such clear relationships. Instead, the nudged experiments
 437 show a zonally symmetric decrease of HCF under QBOW compared to QBOE. This could sug-
 438 gest that the without dynamical feedbacks, the QBO impact is to decrease HCF at equatorial
 439 latitudes.

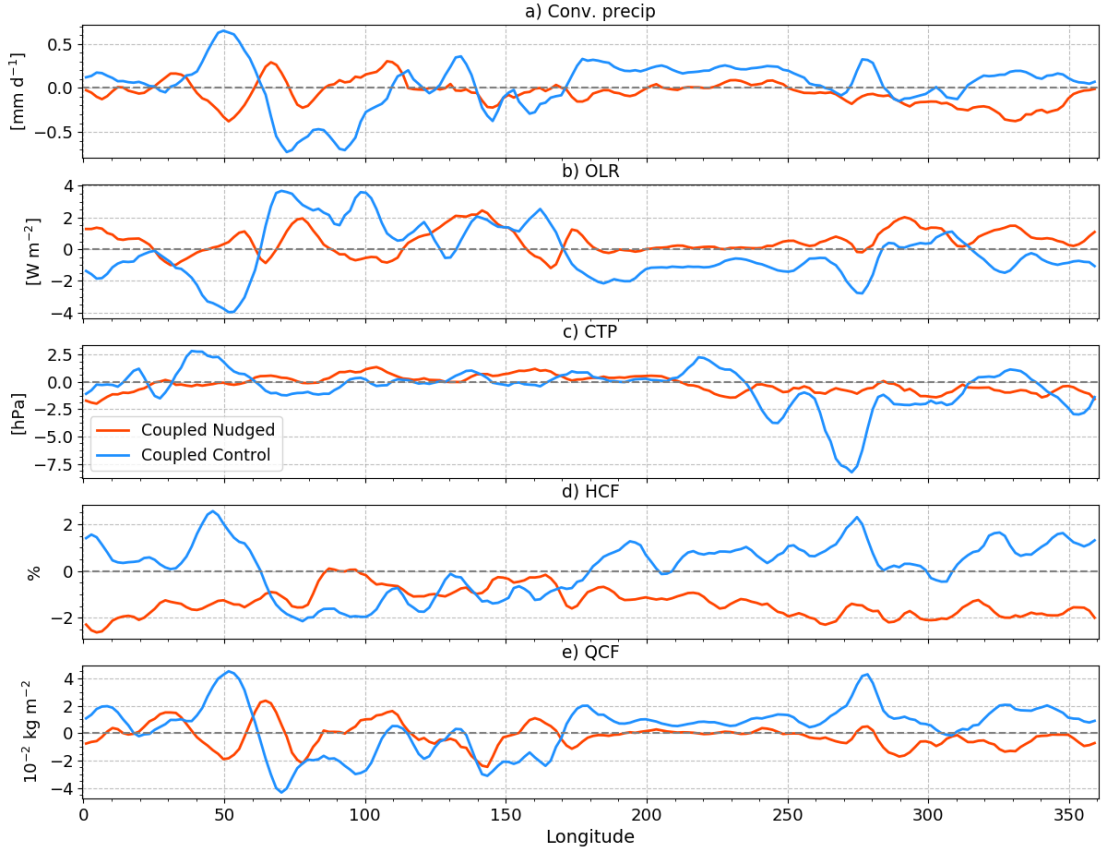


Figure 11. Zonal-mean equatorially averaged [10S-10N] annual-mean differences QBO W-E (during neutral ENSO conditions only) of (a) convective precipitation [mm day^{-1}], (b) OLR [W m^{-2}], (c) cloud top pressure [Pa], (d) high-cloud fraction [%] and (e) ice total content [$10^{-2} \text{ kg m}^{-2}$].

440 In short, this section shows that when the stratosphere is nudged fewer high clouds are found
 441 under QBOW compared to QBOE at equatorial latitudes. In contrast, the control experiments
 442 show zonally asymmetric signals, particularly in the Indian Ocean, which closely follow precip-
 443 itation and OLR anomalies. These results suggest that the interaction between high clouds and
 444 the QBO phase has been modified by the nudging. Despite exhibiting robust zonally symmet-
 445 ric anomalies in HCF, the nudged experiments do not show spatially coherent or robust convec-
 446 tive precipitation differences. This result could suggest that changes to high cloud fraction or ice
 447 content alone are not sufficient for a significant precipitation response.

448 **4 Discussion and conclusions**

449 A set of nudging experiments performed with the MOHC UM was used to investigate three
 450 existing hypotheses that could explain links between the QBO and tropical convection and pre-

451 precipitation. By nudging the zonal wind in the equatorial stratosphere towards ERA5, the UM re-
452 realistically reproduces the observed QBO-related variability in the zonal wind and temperature
453 in the UTLS region. The nudging thus removed the weak QBO amplitude bias in the lower strato-
454 sphere which could modify or weaken QBO tropical surface impacts in GCMs (J. C. K. Lee &
455 Klingaman, 2018; H. Kim, Caron, et al., 2020; Martin et al., 2021a).

456 The analysis of the atmosphere-only experiments has shown that the zonal wind in the equa-
457 torial stratosphere, either nudged or free-running, makes little difference to the simulation of pre-
458 cipitation in the UM with prescribed SSTs as boundary conditions. This result implies that any
459 process that links the QBO to the tropical circulation within the model, such as those diagnosed
460 in García-Franco et al. (2022), requires SSTs to play an active role, either driving the relation-
461 ship or through SST-QBO feedbacks.

462 The role of SST feedbacks for the QBO mechanism was investigated using coupled ocean-
463 atmosphere experiments. In the control experiments, the SSTs over tropical oceans were found
464 to be warmer under QBOW than under QBOE, in agreement with García-Franco et al. (2022).
465 Precipitation patterns in these experiments follow the SSTs with wetter conditions over equa-
466 torial oceans under QBOW compared to QBOE. However, in the nudged ensemble-mean, both
467 SST and precipitation differences were null or close to zero in equatorial regions, meaning that
468 the relationship between the QBO and the tropical surface in the control experiments was muted
469 by the nudging. A closer inspection of other relationships between the QBO and the IOD and
470 ENSO (García-Franco et al., 2022), confirmed that the nudging has notably modified, and in some
471 cases removed, the QBO signal at the tropical surface.

472 One possible explanation for these results is that the simulated QBO-tropical teleconnec-
473 tions are the result of a bottom-up process which is broken when the stratosphere is nudged to-
474 wards a specified state. Since the QBO is tightly coupled to the interaction between convectively
475 triggered waves and the stratospheric mean flow (Baldwin et al., 2001; Y.-H. Kim & Chun, 2015;
476 Geller et al., 2016; Garfinkel et al., 2022), the QBO is modulated by tropical variability such as
477 ENSO events (Schirber, 2015; Serva et al., 2020). Therefore, one could reasonably suspect that
478 the difference between the control and the nudged experiments is simply that waves propagat-
479 ing from the tropical troposphere cannot propagate to the nudged layer in the nudged experi-
480 ments.

481 However, previous studies have found no evidence for an impact from ENSO on to the QBO
482 amplitude and descent rates in the UM (Serva et al., 2020; García-Franco et al., 2022). While

483 tropical waves propagated from the troposphere to the stratosphere are a main control of the QBO
484 characteristics, the impact of upward tropical wave propagation is subtle and does not instan-
485 taneously change the zonal mean wind at 70 hPa (which is our index). This means that the ENSO-
486 QBO relationship in the UM model remains to be explained.

487 Another possibility is that feedbacks that are responsible for the relationships simulated
488 in the control simulations were removed by the nudging. This possibility was investigated using
489 elements from three hypotheses that could explain QBO teleconnections in the tropics: the static
490 stability, the Walker circulation and high cloud feedbacks. The static stability hypothesis sug-
491 gests that the UTLS temperature structure, affected by the QBO on interannual timescales, can
492 modify the strength of convection such that decreased UTLS static stability under QBOE increases
493 convection and precipitation compared to QBOW (Collimore et al., 2003; Liess & Geller, 2012).

494 However, this study shows that the magnitude and sign of the UTLS static stability vari-
495 ability associated with the QBO (Figs. 7 and 8) have no robust relationship with precipitation
496 variability in the deep tropics in the UM. First, the QBO signal in UTLS static stability was found
497 to be zonally symmetric but the QBO signal in precipitation was highly asymmetric. Second, the
498 nudged experiments more than doubled the UTLS static stability variability associated with the
499 QBO, yet the precipitation response to the QBO phase was muted when the nudging was ap-
500 plied. Nevertheless, variability in the UTLS static stability is indeed positively correlated to pre-
501 cipitation variability over tropical oceans (Fig. 8d). The implication from this result is that QBO-
502 related variability in UTLS static stability is not a sufficient process to explain the link between
503 the QBO and tropical convection and other processes amplify or overwhelm the influence of the
504 static stability.

505 A second hypothesis argues that the Walker circulation strength and location is affected
506 by the QBO, which could explain why the precipitation response in the tropics is zonally asym-
507 metric (Hitchman et al., 2021; García-Franco et al., 2022). The coupled experiments showed that
508 the nudging significantly affected the mean-state and variability of the upper branch of the Walker
509 circulation in the Pacific and maritime continent. A weakening of the Walker circulation under
510 QBOW compared to QBOE is diagnosed in observations, the control experiments and other ver-
511 sions of the UM model (Hitchman et al., 2021; García-Franco et al., 2022). However, the QBO-
512 Walker circulation relationship was weakened when the nudging was applied to the model. In
513 fact, the Indian Ocean response even reversed sign relative to the control. One possible expla-
514 nation is that the nudging has overly constrained the upper branch of the Walker circulation, re-

515 moving mean-state biases and, to some extent, the influence from the SSTs on to the 200-100
516 hPa temperature and wind fields (Fig. 9e-f). This result could mean that the Walker circulation
517 plays a role in amplifying local-scale effects of the QBO in a feedback process which was mod-
518 ified by the nudging. used, including cloud fraction and ice cloud content, an Finally, a CRE hy-
519 pothesis has been suggested recently which argues that cirrus clouds play an important role in
520 QBO tropical teleconnections (Sun et al., 2019; Sakaeda et al., 2020; Lin & Emanuel, 2022). This
521 CRE hypothesis could operate at the large-scale, if the QBO modifies the mean-state of clouds
522 in the TTL region (Tseng & Fu, 2017; Sweeney et al., 2022) but also at the convective scale if
523 strength of ascent and vertical advection of water vapour is modified by the QBO (Nie & Sobel,
524 2015; Sakaeda et al., 2020).

525 To investigate this hypothesis, several diagnostics for high clouds were shown to be pos-
526 itively correlated with precipitation changes in the control experiments. In the nudged exper-
527 iments, a robust decreased fraction of high clouds under QBOW compared to QBOE is diagnosed
528 across equatorial regions, which agrees with some observational and modelling evidence (Sun et
529 al., 2019; Sakaeda et al., 2020; Sweeney et al., 2022; Lin & Emanuel, 2022). However, in the nudged
530 experiments differences in high cloud fraction are not related to precipitation or OLR anoma-
531 lies. These results highlight that the simulated QBO teleconnections require tropical stratosphere-
532 troposphere coupling and feedbacks.

533 One possible drawback of the nudging approach employed in this study is that the QBO
534 winds have been nudged to the observations at all longitudes, in contrast to some studies that
535 only nudge the zonal-mean values. While the QBO sets the zonal-mean temperature and wind,
536 the local conditions of clouds, convection and temperature in the tropical UTLS are heavily in-
537 fluenced by feedbacks at the UTLS region involving the horizontal advection of clouds (Lin &
538 Emanuel, 2022), static stability (Nie & Sobel, 2015), or upward wave propagation (Sakaeda et
539 al., 2020; Holt et al., 2022). This means that if the QBO is linked to tropical convection in the
540 UM through the interaction of upward wave propagation and high-clouds, or through large-scale
541 zonal circulations, with the underlying SSTs, our nudging setup was not the appropriate to di-
542 agnose these mechanisms. Based on this hypothesis, the nudging at all longitudes of this study
543 would weaken or even remove the influence of the lower troposphere on the local TTL and mut-
544 ing feedbacks potentially involving large-scale tropical circulations. However, further studies, with
545 different types of nudging or with different models are required to test these hypotheses.

546 **Open Research Section**

547 The reanalysis, observational and CMIP6 data is publicly available (see references in main
548 text). The simulation data will be made publicly available at the time of acceptance.

549 **Acknowledgments**

550 JLGF acknowledges support from an Oxford-Richards Scholarship.

551 **References**

- 552 Adler, R. F., Huffman, G. J., Chang, A., Ferraro, R., Xie, P.-P., Janowiak, J., . . . Nelkin, E.
553 (2003). The version-2 global precipitation climatology project (GPCP) monthly precipita-
554 tion analysis (1979–present). *Journal of hydrometeorology*, *4*(6), 1147–1167.
- 555 Allan, R. P. (2011). Combining satellite data and models to estimate cloud radiative effect
556 at the surface and in the atmosphere. *Meteorological Applications*, *18*(3), 324–333.
- 557 Back, S.-Y., Han, J.-Y., & Son, S.-W. (2020). Modeling evidence of qbo-mjo connection: A
558 case study. *Geophysical Research Letters*, *47*(20), e2020GL089480.
- 559 Baldwin, M., Gray, L., Dunkerton, T., Hamilton, K., Haynes, P., Randel, W., . . . others
560 (2001). The quasi-biennial oscillation. *Reviews of Geophysics*, *39*(2), 179–229.
- 561 Bushell, A. C., Anstey, J. A., Butchart, N., Kawatani, Y., Osprey, S. M., Richter, J. H., . . .
562 Yukimoto, S. (2020). Evaluation of the Quasi-Biennial Oscillation in global climate models
563 for the SPARC QBO-initiative. *Quarterly Journal of the Royal Meteorological Society*,
564 1–31. Retrieved from [https://rmets.onlinelibrary.wiley.com/doi/abs/10.1002/](https://rmets.onlinelibrary.wiley.com/doi/abs/10.1002/qj.3765)
565 [qj.3765](https://doi.org/10.1002/qj.3765) doi: <https://doi.org/10.1002/qj.3765>
- 566 Byrne, M. P., & Zanna, L. (2020). Radiative effects of clouds and water vapor on an axisym-
567 metric monsoon. *Journal of Climate*, *33*(20), 8789–8811.
- 568 Collimore, C. C., Martin, D. W., Hitchman, M. H., Huesmann, A., & Waliser, D. E. (2003).
569 On the relationship between the QBO and tropical deep convection. *Journal of climate*,
570 *16*(15), 2552–2568.
- 571 Davis, S. M., Liang, C. K., & Rosenlof, K. H. (2013). Interannual variability of tropical
572 tropopause layer clouds. *Geophysical Research Letters*, *40*(11), 2862–2866.
- 573 Domeisen, D. I., Garfinkel, C. I., & Butler, A. H. (2019). The teleconnection of El Niño
574 Southern Oscillation to the stratosphere. *Reviews of Geophysics*, *57*(1), 5–47.
- 575 García-Franco, J. L., Gray, L. J., Osprey, S., Chadwick, R., & Martin, Z. (2022). The trop-

- 576 ical route of quasi-biennial oscillation (qbo) teleconnections in a climate model. *Weather*
577 *and Climate Dynamics*, 3(3), 825–844. doi: 10.5194/wcd-3-825-2022
- 578 Garfinkel, C. I., Gerber, E. P., Shamir, O., Rao, J., Jucker, M., White, I., & Paldor, N.
579 (2022). A qbo cookbook: Sensitivity of the quasi-biennial oscillation to resolution, resolved
580 waves, and parameterized gravity waves. *Journal of Advances in Modeling Earth Systems*,
581 14(3), e2021MS002568.
- 582 Garfinkel, C. I., & Hartmann, D. L. (2011). The influence of the quasi-biennial oscillation
583 on the troposphere in winter in a hierarchy of models. Part II: Perpetual winter WACCM
584 runs. *Journal of the Atmospheric Sciences*, 68(9), 2026–2041.
- 585 Geller, M. A., Zhou, T., & Yuan, W. (2016). The qbo, gravity waves forced by tropical con-
586 vection, and enso. *Journal of Geophysical Research: Atmospheres*, 121(15), 8886–8895.
- 587 Giorgetta, M. A., Bengtsson, L., & Arpe, K. (1999). An investigation of QBO signals in the
588 east Asian and Indian monsoon in GCM experiments. *Climate dynamics*, 15(6), 435–450.
- 589 Gray, L., Brown, M., Knight, J., Andrews, M., Lu, H., O’Reilly, C., & Anstey, J. (2020).
590 Forecasting extreme stratospheric polar vortex events. *Nature communications*, 11(1),
591 1–9.
- 592 Gray, L. J., Anstey, J. A., Kawatani, Y., Lu, H., Osprey, S., & Schenzinger, V. (2018).
593 Surface impacts of the Quasi Biennial Oscillation. *Atmospheric Chemistry and Physics*,
594 18(11), 8227–8247. doi: 10.5194/acp-18-8227-2018
- 595 Gray, W. M. (1984). Atlantic seasonal hurricane frequency. Part I: El Niño and 30 mb quasi-
596 biennial oscillation influences. *Monthly Weather Review*, 112(9), 1649–1668.
- 597 Gray, W. M., Sheaffer, J. D., & Knaff, J. A. (1992). Influence of the stratospheric QBO on
598 ENSO variability. *Journal of the Meteorological Society of Japan. Ser. II*, 70(5), 975–995.
- 599 Hartmann, D. L., & Berry, S. E. (2017). The balanced radiative effect of tropical anvil
600 clouds. *Journal of Geophysical Research: Atmospheres*, 122(9), 5003–5020.
- 601 Haynes, P., Hitchcock, P., Hitchman, M., Yoden, S., Hendon, H., Kiladis, G., . . . Simpson,
602 I. (2021). The influence of the stratosphere on the tropical troposphere. *Journal of the*
603 *Meteorological Society of Japan. Ser. II*.
- 604 Hendon, H. H., & Abhik, S. (2018). Differences in vertical structure of the madden-julian
605 oscillation associated with the quasi-biennial oscillation. *Geophysical Research Letters*,
606 45(9), 4419–4428.
- 607 Hersbach, H., Bell, B., Berrisford, P., Hirahara, S., Horányi, A., Muñoz-Sabater, J., . . .
608 Thépaut, J.-N. (2020). The ERA5 global reanalysis. *Quarterly Journal of the Royal*

- 609 *Meteorological Society*, 146(730), 1999–2049. doi: 10.1002/qj.3803
- 610 Hitchman, M. H., Yoden, S., Haynes, P. H., Kumar, V., & Tegtmeier, S. (2021). An ob-
 611 servational history of the direct influence of the stratospheric quasi-biennial oscillation on
 612 the tropical and subtropical upper troposphere and lower stratosphere. *Journal of the*
 613 *Meteorological Society of Japan. Ser. II.*
- 614 Holt, L. A., Lott, F., Garcia, R. R., Kiladis, G. N., Cheng, Y.-M., Anstey, J. A., ... others
 615 (2022). An evaluation of tropical waves and wave forcing of the qbo in the qboi models.
 616 *Quarterly Journal of the Royal Meteorological Society*, 148(744), 1541–1567.
- 617 Hu, Z.-Z., Huang, B., Kinter, J. L., Wu, Z., & Kumar, A. (2012). Connection of the strato-
 618 spheric QBO with global atmospheric general circulation and tropical SST. Part II: inter-
 619 decadal variations. *Climate dynamics*, 38(1), 25–43.
- 620 Kennedy, J. J., Rayner, N., Atkinson, C., & Killick, R. (2019). An ensemble data set of sea
 621 surface temperature change from 1850: The met office hadley centre hadsst. 4.0. 0.0 data
 622 set. *Journal of Geophysical Research: Atmospheres*, 124(14), 7719–7763.
- 623 Kim, H., Caron, J. M., Richter, J. H., & Simpson, I. R. (2020). The lack of QBO-MJO
 624 Connection in CMIP6 Models. *Geophysical Research Letters*, 47(11), e2020GL087295.
 625 (e2020GL087295 2020GL087295) doi: 10.1029/2020GL087295
- 626 Kim, H., Son, S.-W., & Yoo, C. (2020). Qbo modulation of the mjo-related precipitation in
 627 east asia. *Journal of Geophysical Research: Atmospheres*, 125(4), e2019JD031929.
- 628 Kim, Y.-H., & Chun, H.-Y. (2015). Contributions of equatorial wave modes and parameter-
 629 ized gravity waves to the tropical qbo in hadgem2. *Journal of Geophysical Research: At-*
 630 *mospheres*, 120(3), 1065–1090.
- 631 Lee, J. C. K., & Klingaman, N. P. (2018). The effect of the quasi-biennial oscillation on
 632 the Madden–Julian oscillation in the Met Office Unified Model Global Ocean Mixed Layer
 633 configuration. *Atmospheric Science Letters*, 19(5), e816. doi: 10.1002/asl.816
- 634 Lee, J.-H., Kang, M.-J., & Chun, H.-Y. (2019). Differences in the tropical convective activi-
 635 ties at the opposite phases of the quasi-biennial oscillation. *Asia-Pacific Journal of Atmo-*
 636 *spheric Sciences*, 55(3), 317–336.
- 637 Liess, S., & Geller, M. A. (2012). On the relationship between qbo and distribution of tropi-
 638 cal deep convection. *Journal of Geophysical Research: Atmospheres*, 117(D3).
- 639 Lim, Y., & Son, S.-W. (2022). Qbo wind influence on mjo-induced temperature anomalies in
 640 the upper troposphere and lower stratosphere in an idealized model. *Journal of the Atmo-*
 641 *spheric Sciences.*

- 642 Lin, J., & Emanuel, K. (2022). Stratospheric modulation of the mjo through cirrus cloud
643 feedbacks. *Journal of the Atmospheric Sciences*.
- 644 Martin, Z., Orbe, C., Wang, S., & Sobel, A. (2021a). The MJO–QBO Relationship in a
645 GCM with Stratospheric Nudging. *Journal of Climate*, *34*(11), 4603–4624.
- 646 Martin, Z., Sobel, A., Butler, A., & Wang, S. (2021c). Variability in qbo temperature
647 anomalies on annual and decadal time scales. *Journal of Climate*, *34*(2), 589–605.
- 648 Martin, Z., Son, S.-W., Butler, A., Hendon, H., Kim, H., Sobel, A., . . . Zhang, C. (2021b).
649 The influence of the quasi-biennial oscillation on the madden–julian oscillation. *Nature Re-*
650 *views Earth & Environment*, 1–13.
- 651 Martin, Z., Wang, S., Nie, J., & Sobel, A. (2019, 02). The Impact of the QBO on MJO Con-
652 vection in Cloud-Resolving Simulations. *Journal of the Atmospheric Sciences*, *76*(3), 669-
653 688.
- 654 Menary, M. B., Kuhlbrodt, T., Ridley, J., Andrews, M. B., Dimdore-Miles, O. B., Deshayes,
655 J., . . . Xavier, P. (2018). Preindustrial control simulations with HadGEM3-GC3. 1 for
656 CMIP6. *Journal of Advances in Modeling Earth Systems*, *10*(12), 3049–3075.
- 657 Nie, J., & Sobel, A. H. (2015). Responses of tropical deep convection to the QBO: Cloud-
658 resolving simulations. *Journal of the Atmospheric Sciences*, *72*(9), 3625–3638.
- 659 Rao, J., Garfinkel, C. I., & White, I. P. (2020). How does the quasi-biennial oscillation affect
660 the boreal winter tropospheric circulation in cmip5/6 models? *Journal of Climate*, *33*(20),
661 8975–8996.
- 662 Richter, J. H., Anstey, J. A., Butchart, N., Kawatani, Y., Meehl, G. A., Osprey, S., & Simp-
663 son, I. R. (2020). Progress in simulating the Quasi-Biennial Oscillation in CMIP models.
664 *Journal of Geophysical Research: Atmospheres*, *125*(8), e2019JD032362. (e2019JD032362
665 10.1029/2019JD032362)
- 666 Sakaeda, N., Dias, J., & Kiladis, G. N. (2020). The unique characteristics and potential
667 mechanisms of the mjo-qbo relationship. *Journal of Geophysical Research: Atmospheres*,
668 *125*(17), e2020JD033196.
- 669 Schenzinger, V., Osprey, S., Gray, L., & Butchart, N. (2017). Defining metrics of the Quasi-
670 Biennial oscillation in global climate models. *Geoscientific Model Development*, *10*(6).
- 671 Schirber, S. (2015). Influence of ENSO on the QBO: Results from an ensemble of idealized
672 simulations. *Journal of Geophysical Research: Atmospheres*, *120*(3), 1109–1122.
- 673 Serva, F., Anstey, J. A., Bushell, A. C., Butchart, N., Cagnazzo, C., Gray, L., . . . Simpson,
674 I. R. (2022). The impact of the QBO on the region of the tropical tropopause in QBOi

- 675 models: present-day simulations. *Quarterly Journal of the Royal Meteorological Society*,
676 *148*(745), 1945-1964. doi: <https://doi.org/10.1002/qj.4287>
- 677 Serva, F., Cagnazzo, C., Christiansen, B., & Yang, S. (2020). The influence of enso events on
678 the stratospheric qbo in a multi-model ensemble. *Climate Dynamics*, *54*(3), 2561–2575.
- 679 Son, S.-W., Lim, Y., Yoo, C., Hendon, H. H., & Kim, J. (2017). Stratospheric control of the
680 Madden–Julian oscillation. *Journal of Climate*, *30*(6), 1909–1922.
- 681 Storkey, D., Blaker, A. T., Mathiot, P., Megann, A., Aksenov, Y., Blockley, E. W., ... others
682 (2018). UK Global Ocean GO6 and GO7: A traceable hierarchy of model resolutions.
683 *Geoscientific Model Development*, *11*(8), 3187–3213.
- 684 Sun, L., Wang, H., & Liu, F. (2019). Combined effect of the qbo and enso on the mjo. *Atmo-*
685 *spheric and Oceanic Science Letters*, *12*(3), 170–176.
- 686 Sweeney, A. J., Fu, Q., Pahlavan, H. A., & Haynes, P. (2022, aug). Seasonality of the QBO
687 impact on equatorial clouds. *ESSOAR*. Retrieved from [https://doi.org/10.1002/](https://doi.org/10.1002/2Fessoar.10512278.1)
688 [2Fessoar.10512278.1](https://doi.org/10.1002/2Fessoar.10512278.1) doi: 10.1002/essoar.10512278.1
- 689 Tegtmeier, S., Anstey, J., Davis, S., Ivanciu, I., Jia, Y., McPhee, D., & Pilch Kedzierski, R.
690 (2020). Zonal Asymmetry of the QBO Temperature Signal in the Tropical Tropopause
691 Region. *Geophysical Research Letters*, *47*(24), e2020GL089533. (e2020GL089533
692 2020GL089533) doi: <https://doi.org/10.1029/2020GL089533>
- 693 Telford, P., Braesicke, P., Morgenstern, O., & Pyle, J. (2008). Description and assessment of
694 a nudged version of the new dynamics unified model. *Atmospheric Chemistry and Physics*,
695 *8*(6), 1701–1712.
- 696 Trenberth, K. E. (1997). The definition of el nino. *Bulletin of the American Meteorological*
697 *Society*, *78*(12), 2771–2778.
- 698 Tseng, H.-H., & Fu, Q. (2017). Temperature control of the variability of tropical tropopause
699 layer cirrus clouds. *Journal of Geophysical Research: Atmospheres*, *122*(20), 11–062.
- 700 Walters, D., Boutle, I., Brooks, M., Melvin, T., Stratton, R., Vosper, S., ... Xavier, P.
701 (2019). The Met Office Unified Model global atmosphere 7.0/7.1 and JULES global land
702 7.0 configurations. *Geoscientific Model Development*, *12*(5), 1909–1963.
- 703 Yoo, C., & Son, S.-W. (2016). Modulation of the boreal wintertime madden-julian oscillation
704 by the stratospheric quasi-biennial oscillation. *Geophysical Research Letters*, *43*(3), 1392–
705 1398.

Supporting Information for ”Understanding the mechanisms for tropical surface impacts of the quasi-biennial oscillation (QBO)”

Jorge L. García-Franco^{1,2}, Lesley J. Gray^{1,3}, Scott Osprey^{1,3}, Robin

Chadwick^{4,5} and Jonathan Lin²

¹Atmospheric, Oceanic and Planetary Physics, University of Oxford

²Lamont-Doherty Earth Observatory, Columbia University, NY

³National Centre for Atmospheric Science, Oxford, United Kingdom

⁴Met Office Hadley Centre, UK

⁵Global Systems Institute, Department of Mathematics, University of Exeter, Exeter, UK

Contents of this file

1. Figures S1 to S6.

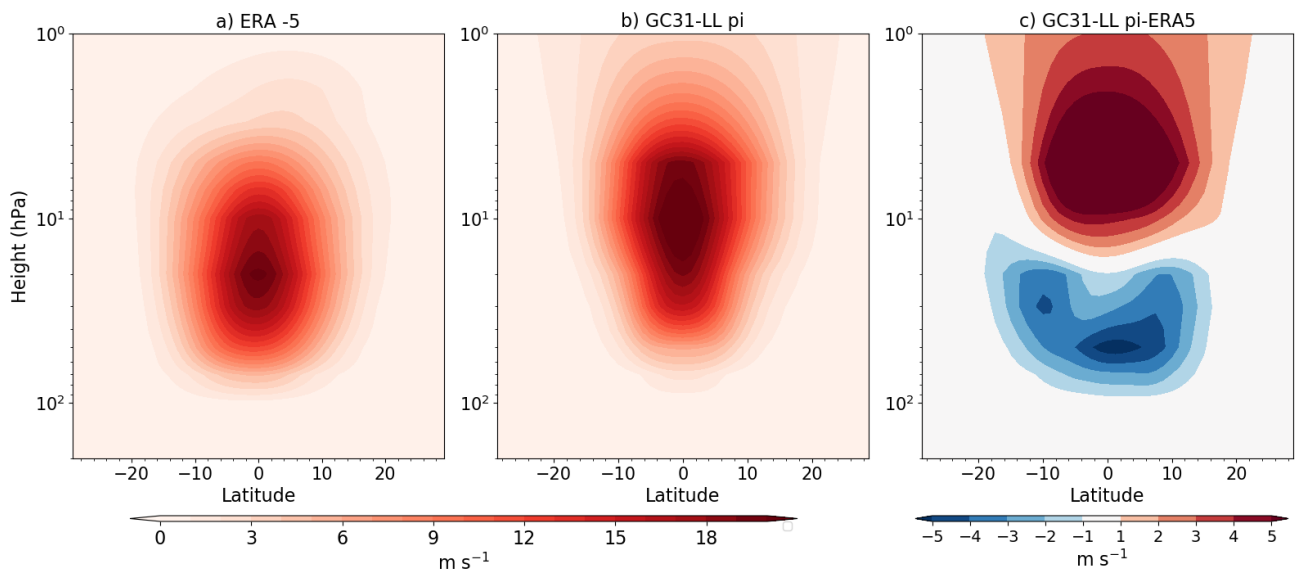


Figure S1. Latitude-pressure plot of the amplitude [m s^{-1}] of the QBO. Obtained from the zonal mean zonal wind fourier spectrum magnitude within the QBO periods, as in ? (?).

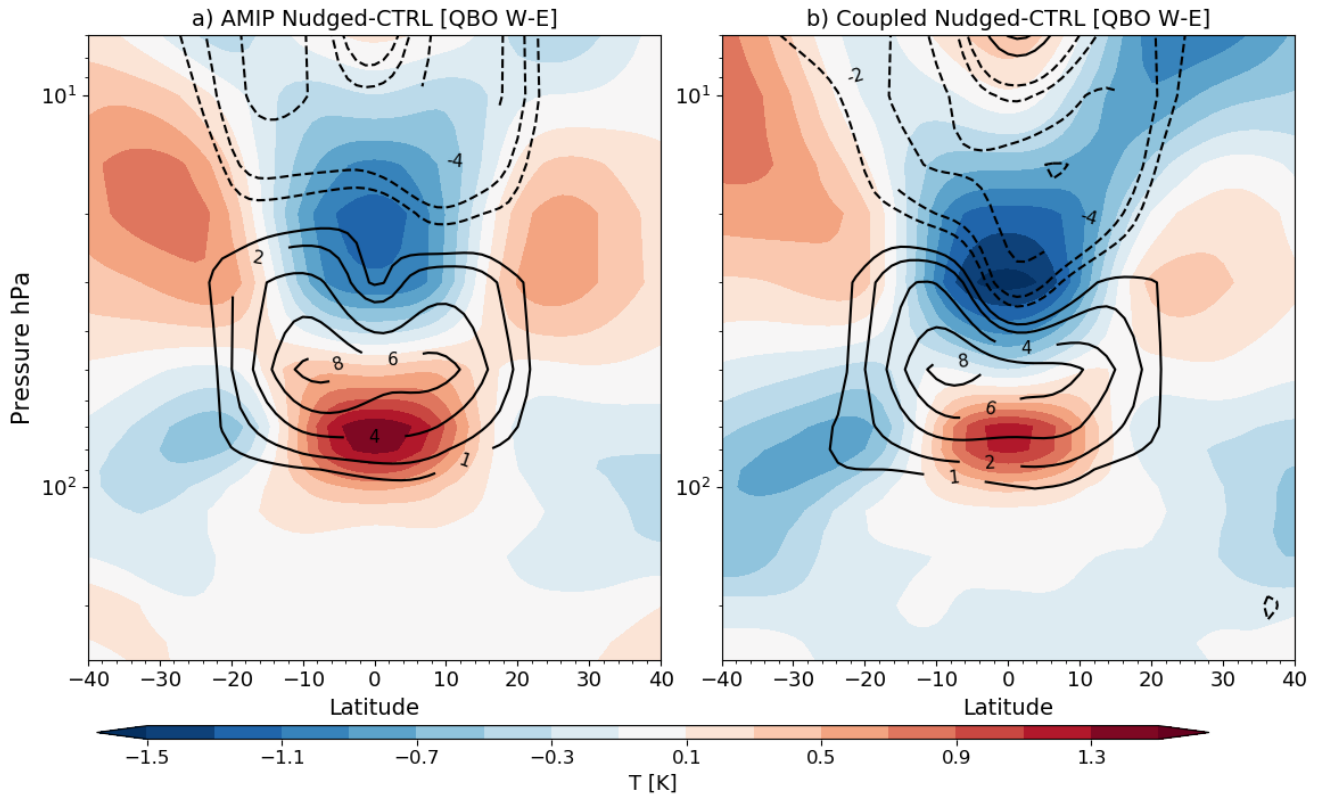


Figure S2. Differences in the QBO-related (W-E) variability in zonal mean zonal wind and temperature in (a) AMIP and (b) Coupled experiments between runs with and without nudging.

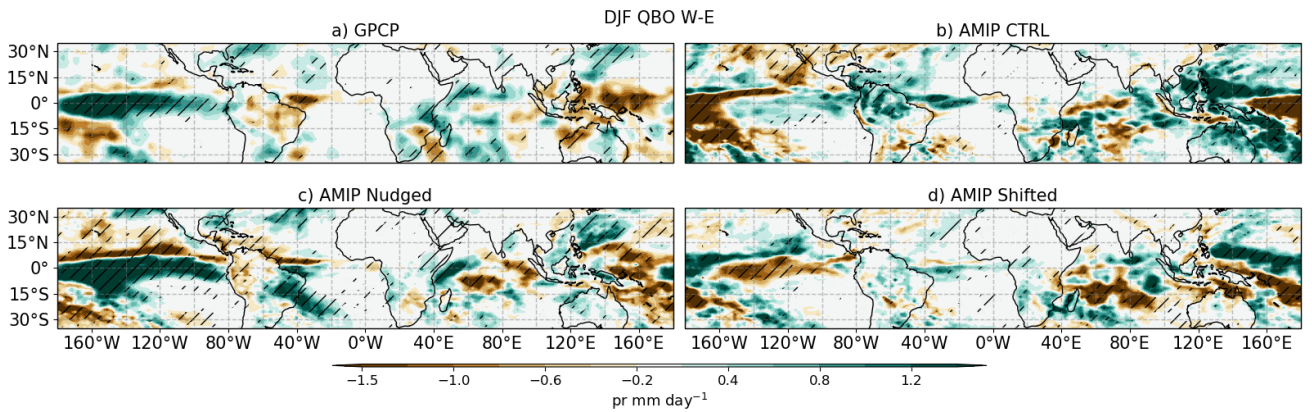


Figure S3. As in Fig. 3 of the main manuscript but for the DJF season.

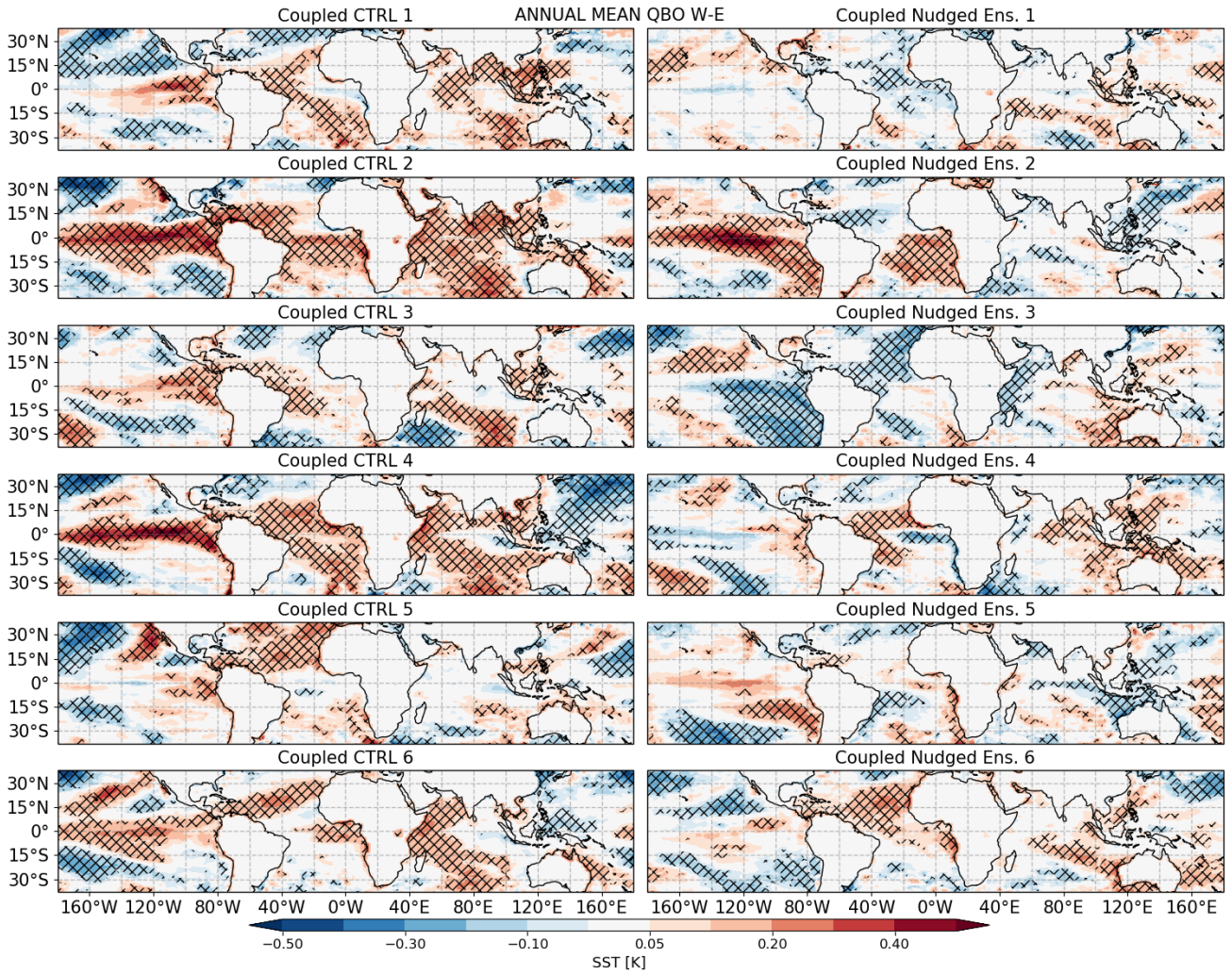


Figure S4. Annual mean SST differences (QBO W-E) in Coupled Control (left) and Coupled Nudged (right) ensemble members. Hatching denotes significance to the 95% confidence level according to a bootstrapping with replacement test.

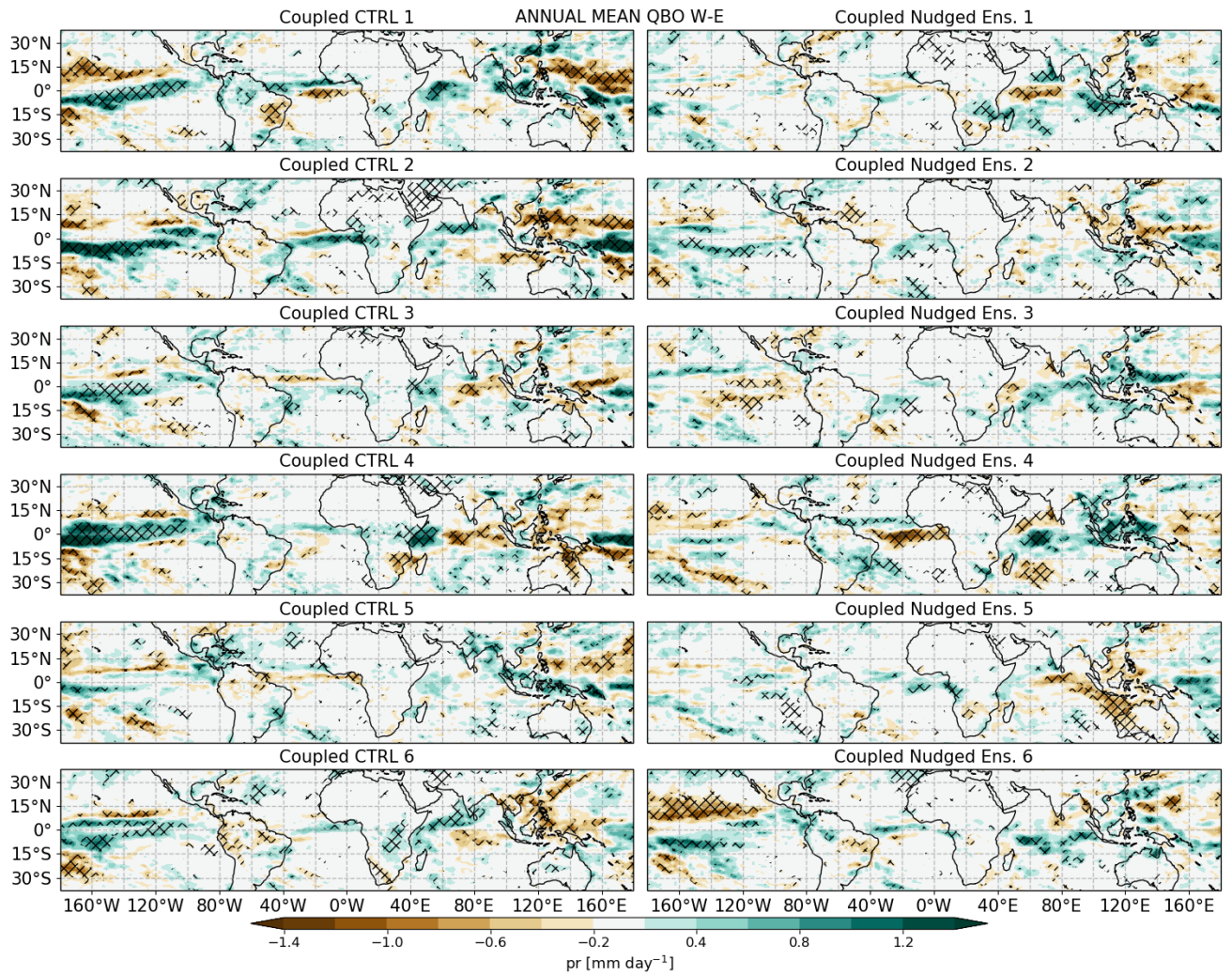


Figure S5. As in Fig. S4 but for precipitation.

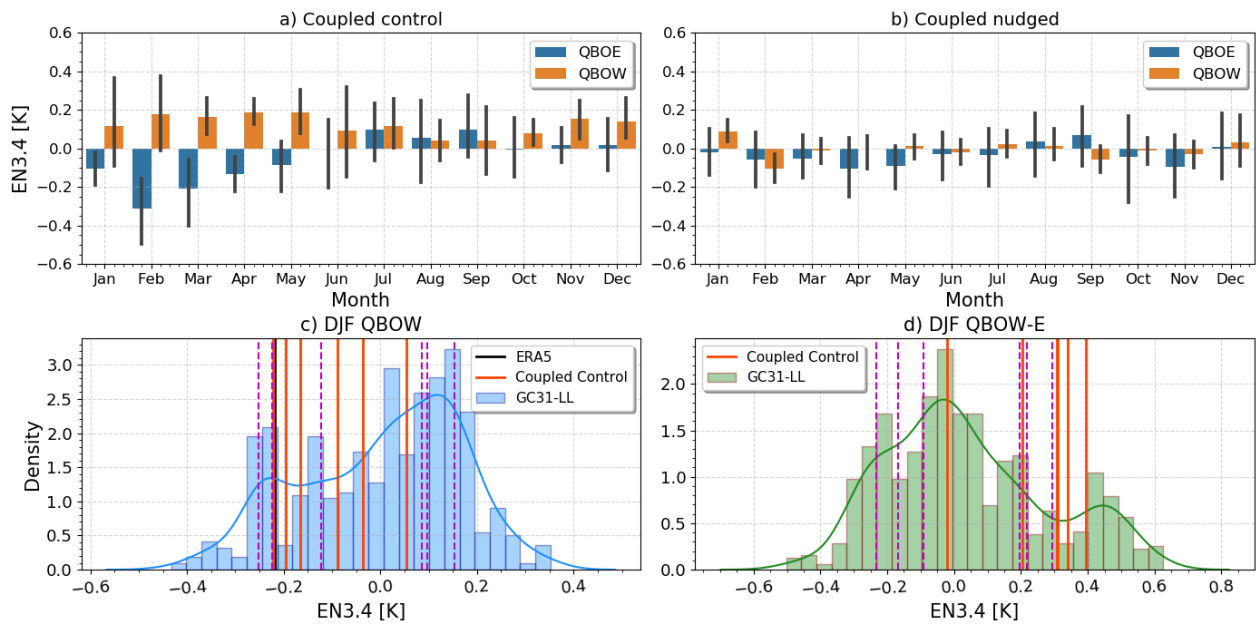


Figure S6. As in Fig. 7 of the main manuscript but for the EN3.4 index.